

MATHEMATICAL MODELING OF MALTOSE UPTAKE
SYSTEM IN E. COLI USING NANODISC FLUORESCENCE
QUENCHING DATA

by

Rebecca Marie Hiller

B.Sc., B.A., Humboldt State University, 2009

A THESIS SUBMITTED IN PARTIAL FULFILLMENT OF THE
REQUIREMENTS FOR THE DEGREE OF

MASTER OF SCIENCE
in
THE FACULTY OF GRADUATE STUDIES

(Mathematics)

THE UNIVERSITY OF BRITISH COLUMBIA
(Vancouver)
April 2013

©Rebecca Marie Hiller 2013

Abstract

Recent data measured in nanodiscs conflicts with the standard theory of maltose transport in the MalE-MalFGK₂ uptake system found in *E. coli*. Nanodisc fluorescence quenching data suggest an alternate pathway in which unliganded MalE binds the P-open transporter, facilitating maltose acquisition. Nanodisc data also indicate that MalE regulates maltose uptake at high concentrations. We analyzed four mathematical models of the maltose uptake system: the distinct standard and alternate models, and two integrated models. Nanodisc fluorescence quenching data and nonlinear regression analysis were used to fit equilibrium constants and kinetic rates. The flux through each pathway in an integrated model was calculated using asymptotic analysis and fit parameter values. We conclude that it is likely that transport occurs when liganded MalE associates to a P-open conformation of MalFGK₂, rather than binding to the P-closed transporter as suggested by the standard model. The standard pathway was calculated to be negative, i.e. to occur in reverse as a means of regulating maltose uptake at high concentration. This analysis conflicts with the standard model in which liganded MalE binds to a closed transporter and triggers an opening of the transporter proteins which in turn open the liganded MalE. The analysis also found that a relatively small amount of maltose transport may occur through the alternate pathway involving unliganded MalE.

Contents

Abstract	ii
Contents	iii
List of Tables	vi
List of Figures	vii
Acknowledgements	viii
Dedication	ix
1 Introduction	1
1.1 ABC Transporters	1
1.2 Maltose Uptake System in E. Coli	2
1.3 Standard Model	3
1.3.1 Supporting Evidence	3
1.3.2 Contradicting Evidence	4
1.4 Alternate Model of Maltose Transport	4
1.5 Previous Modeling of Maltose Uptake System	5

2	Mathematical Models	6
2.1	Standard Model	9
2.2	Alternate Model	9
2.3	Comprehensive Model	12
2.4	Full Model	15
3	Experimental Data	21
3.1	Fluorescence Quenching Experiments	22
3.2	Equilibrium Data	22
3.3	Time-Dependent Data	22
3.4	ATPase Experiments	25
3.5	Fit Methods	25
3.6	Fit Analysis	25
4	Nonlinear Regression Fit	27
4.1	Equilibrium Data Fit	27
4.1.1	Standard Model	27
4.1.2	Alternate Model	28
4.1.3	Comprehensive Model	31
4.1.4	Full Model	32
4.2	Time-Dependent Data Fit	40
4.2.1	In the limit $K_1 \rightarrow 0$	40
4.2.2	Fixed K_1, k_1^+	41

4.3	ATPase Data Fit	42
5	Model Comparison	45
5.1	Standard vs. Alternate	45
5.2	Alternate vs. Comprehensive	46
5.3	Comprehensive vs. Full	47
6	Maltose Transport in Comprehensive Model	48
6.1	Analysis of Flux	48
6.2	Further ATPase Results	52
7	Discussion	53
	Bibliography	55
A	Standard Model	57
B	Alternate Model	59
C	Comprehensive Model	61
D	Full Model	66
E	F-test	69
F	Flux Calculation	70

List of Tables

2.1	Model states	8
2.2	Additional Full model state	9
2.3	Kinetic rates and reactions	18
2.4	Additional kinetic parameters and reactions for the Full model	19
2.5	Equilibrium parameters and reactions	20
4.1	Equilibrium fit values for Standard and Alternate models	30
4.2	Equilibrium fit to Comprehensive model, $K_1 = 0.01$	34
4.3	Equilibrium fit to Comprehensive model, $K_1 = 0.1$	35
4.4	Equilibrium fit to Comprehensive model, $K_1 = 1$	36
4.5	Equilibrium fit to Comprehensive model, $K_1 = 100$	37
4.6	Equilibrium fit values for Comprehensive model, $K_1 \rightarrow 0$	37
4.7	Equilibrium fit to Full model	40
4.8	Time-dependent fit	43
5.1	SSR for equilibrium fits	46
E.1	F-test values	69

List of Figures

1.1	ABC transporter diagram	1
1.2	MalE diagram	2
2.1	Standard model diagram	10
2.2	Alternative model diagram	13
2.3	Comprehensive model diagram	14
2.4	Full model diagram	17
3.1	Equilibrium data	23
3.2	Time-dependent data	24
4.1	Equilibrium fit (Comprehensive vs. Alternate vs. Standard)	33
4.2	Equilibrium fit (Full vs. Comprehensive)	38
4.3	Time-dependent fit	44
6.1	Flux for $K_1 \leq 1$	51
6.2	Flux for $K_1 = 100$	51
6.3	ATPase results	52

Acknowledgements

I am very grateful to the faculty and staff at the UBC, for all of their support during my graduate program. I especially want to thank my advisor, Dr. Eric Cytrynbaum, for all of the valuable insight and encouragement throughout this process.

Many thanks to Dr. Franck Duong and Huan Bao in the Department of Biochemistry at UBC for involving us in your exciting research and providing the experimental data for this analysis.

I also want to thank Dr. Dan Coombs for his time and contribution in reading my thesis, his excellent teaching, motivating research, and for always being so helpful.

I have to thank Dr. Leah Keshet for being such an inspiration before and after I came to UBC, and for all of her support and advice.

I owe special thanks to Kelly Paton, for all of the moral support and academic encouragement. I also want to thank Erin Moulding for her constant support and friendship since day one of the program.

Special thanks to my parents, and parents-in-law, for all of your support with my education. I also cannot thank my husband enough for his endless support and confidence in my success, and for moving his life to Canada so I could attend UBC.

Dedicated to Scott

Chapter 1

Introduction

1.1 ABC Transporters

ATP binding cassette (ABC) transporters occur in both eukaryotic and prokaryotic organisms. ABC transporters consist of two ABC domains and two membrane-spanning (transmembrane) domains, as shown in Figure 1.1. The ABC domains are nucleotide binding domains, binding and hydrolyzing ATP to energize unidirectional substrate transport. Substrate transport occurs through a channel formed by the membrane-spanning domains [2]. The ABC transporter domains alternate between two conformations: P-closed (inward facing to the cytosol) and P-open (outward facing to the periplasm) [2].

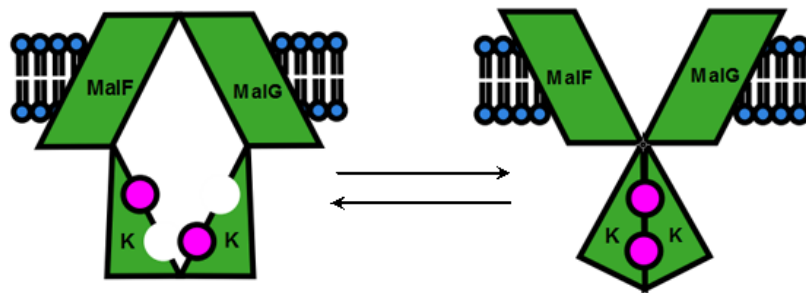


Figure 1.1: Diagram of the P-closed (left) and P-Open (right) conformations of MalFGK₂, an ABC transporter with two membrane-spanning domains (MalF and MalG) and two ABC domains (K), also known as nucleotide binding domains.

ABC transporters facilitate the translocation of various substrates across cell or organelle membranes. Eukaryotic and bacterial ABC transporters mostly differ in both the type of substrate transported, and the direction of transport. Most eukaryotic ABC transporters export hydrophobic molecules from the cytoplasm. Bacterial ABC transporters, however, predominantly import nutrients into the cytoplasm. The import of these nutrients require specific binding proteins, which have been proposed to deliver the nutrients to the transporter [2].

Specifically, there is a class of binding protein-dependent transport systems primarily found in Gram-negative enteric bacteria. These transport systems are specific for sugars, amino acids, and ions [7]. In particular, we consider the binding-protein dependent maltose transport system in the bacteria *E. Coli*.

1.2 Maltose Uptake System in *E. Coli*

MalFGK₂ is a bacterial ABC importer and binding protein-dependent transport system that specifically imports the nutrient maltose in *Escherichia Coli*. MalFGK₂ is composed of 3 proteins: MalF and MalG (the transmembrane proteins) and MalK (the ATP-binding cassette dimer, also called the ATP interface), as seen in Figure 1.1. Maltose transport is dependent upon a substrate-binding protein, MalE, found in the periplasmic region of the bacterial cell [3].

MalE is a protein consisting of two symmetrical lobes that rotate toward each other to capture maltose with high-affinity, as shown in Figure 1.2. This is referred to as the closed-liganded conformation of MalE [3]. MalE is found in the periplasm, and is known to be essential for efficient MalFGK₂ import of maltose.

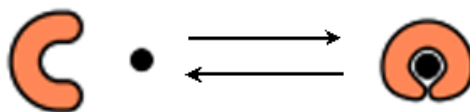


Figure 1.2: MalE reversibly binds to maltose to form closed-liganded MalE.

1.3 Standard Model

The standard model of maltose uptake characterizes MalE as a type of shuttle, delivering maltose to MalFGK₂. The association of maltose-bound MalE is assumed to trigger the conformation change from the P-closed transporter to the P-open transporter [3]. Maltose is subsequently delivered to the open transporter and MalE dissociates upon hydrolysis and transport to return to the periplasm. Recent experimental evidence instead suggests that unliganded MalE binds to the P-open conformation of MalFGK₂, stabilizing or activating the transporter [1].

1.3.1 Supporting Evidence

The standard model has been supported by crystallographic and biochemical analysis. An intermediate of the maltose uptake system has been crystallized which consists of intact MalFGK₂ in complex with MalE, maltose, and ATP [4]. The maltose appears at the interface of the MalF-MalG subunits, about halfway into the lipid bilayer. The MalE is bound to the MalFGK₂ in the open conformation, which has been argued to act as a cap on the transporter to ensure import of the maltose [4]. This intermediate was captured by blocking ATP hydrolysis with a mutation, such that the ATP-binding cassette dimer is captured in an ATP-bound, closed conformation [4]. This transition state is consistent with the standard model pathway of transport, although not uniquely so.

The maltose transporter has also been crystallized in an intermediate step between the P-closed and P-open conformations. It was found that interactions with maltose-bound MalE in the periplasm induces a partial closure of the MalK dimer in the cytoplasm and corresponding opening of the transmembrane domain, in the presence of nucleotides [5]. Furthermore, in the absence of MalE the transporter was crystallized in a P-closed resting state. This supports the assumption that liganded MalE triggers the conformation change to an open transporter state, however it was not shown that MalE without maltose does not induce the same intermediate state [5].

Additionally, an EPR spectroscopy analysis was used to conclude that ligand-bound MalE is needed for the closure of the MalK dimer in the presence of ATP [6].

1.3.2 Contradicting Evidence

There is experimental evidence which contradicts the assumptions of the standard model. A mutant MalFGK₂ which transports lactose instead of maltose was found to still be dependent on MalE for activity, even though MalE does not bind lactose [7]. This suggests that although MalE is critical for transport it may not in fact act as a shuttle for the substrate.

It was also determined that MalE can inhibit transport in excess when maltose is held at sub-stoichiometric levels [8]. The standard model would predict that an increased concentration of MalE would increase transport, as there would be a higher concentration of liganded E_m to stimulate MalFGK₂ to open. If liganded MalE were required to initiate maltose transport, it would be expected that closed-liganded MalE would have a high affinity for the transporter. However, it was reported to have a low affinity for the transporter, 50-100 μM [9]. This further suggests that the underlying assumptions of the standard model may conflict with experimental evidence.

Nanodisc experiments have shown that the open, unliganded conformation of MalE has a high affinity for the open conformation of MalFGK₂. These experiments also showed that MalE with a high affinity for maltose has a low transport rate while MalE with a low affinity for maltose has a high transport rate [1]. An alternate pathway has been suggested to justify these results in which the unliganded MalE plays a critical role for transport.

1.4 Alternate Model of Maltose Transport

In contrast to the standard model, and in support of previous modeling suggesting that unliganded MalE does associate with the transporter [8], an alternate theory of maltose transport has been proposed [1]. In what we will refer to as the Alternate model, unliganded MalE binds with high affinity to MalFGK₂, thus increasing the affinity of the complex for maltose, to facilitate the acquisition of maltose. The Alternate model of maltose transport is supported by experimental data obtained using detergents, liposomes, and nanodisc experiments to investigate MalFGK₂ [1]. Experimental data were used to conclude that transporter-bound MalE facilitates the acquisition of the sugar at low concentrations, while at high sugar concentrations the MalE can bind to maltose and dissociate [1]. This allosteric regulation of maltose therefore limits the overall rate to transport.

1.5 Previous Modeling of Maltose Uptake System

A basic standard model for the maltose uptake system has been proposed and analyzed [8]. The following reactions were included:

$M + E \rightleftharpoons E_m$ where M is the substrate (maltose), E is the binding protein, and E_m is the closed, liganded binding protein.

$E_m + A \rightleftharpoons D \rightarrow A + E$, where A is the MalFGK₂ transporter, D is the complex formed when MalGK₂ binds to the closed liganded binding protein.

These two reactions characterize the standard model. This model was taken a step further to allow for unliganded binding protein to bind to the transporter. This adds the reaction:

$A + E \rightleftharpoons G$, where G is the MalFGK₂ complex with the unliganded binding protein.

From this model it was concluded that (at least in the case of the maltose uptake system) it was likely that both the liganded and unliganded conformations of MalE associate with the transporter. A later extension of this model gave further evidence that both binding protein conformations bind to the transporter. The above model was fit to experimental data in which maltose transport was measured in the presence of constant maltose, but varying binding protein concentration [8].

This model analysis supports the theory that both liganded and unliganded MalE bind to the transporter. However, the model does not distinguish between the open and closed conformations of MalFGK₂, and therefore does not give insight into whether liganded MalE binds to the closed transporter to trigger a conformational change. This model analysis does not give insight into the role of unliganded MalE in transport.

Chapter 2

Mathematical Models

We consider four biochemical reaction networks and their associated ordinary differential equation models for the maltose uptake system in *E. coli*. We refer to these four models as the Standard, Alternate, Comprehensive, and Full models. Table 2.2 gives the symbols used for concentrations of MalFGK₂ transporter states, binding protein (MalE) states, and substrate (maltose) for the four models.

We assume that the concentration of maltose in the periplasm is large relative to the concentration of transporter and binding protein. We therefore make the simplifying assumption that maltose concentration is approximately constant. All concentrations of transporter states and binding protein states are assumed to vary with time when systems are not at equilibrium.

A further model assumption is that nucleotides are required to close the ATP interface resulting in a P-open transporter conformation [5]. Therefore in the absence of nucleotides, we assume that only P-closed (ATP interface open) transporter states are possible and that hydrolysis is inhibited.

In the presence of AMP-PNP, a non-hydrolysable ATP analog, we assume that the ATP interface can close but cannot hydrolyze. This stabilizes the P-open conformation of the transporter. We consider two cases in the presence of AMP-PNP. The simpler case is that all ATP interfaces bind and remain closed in the presence of saturating AMP-PNP, in which case we assume that only P-open transporter states are possible. In the more general case we allow for both P-open and P-closed transporter states in the presence of AMP-PNP (only hydrolysis is inhibited).

Both the Standard and Alternate models are nested within the Comprehensive model as

seen in Figure 2.3. The Comprehensive model is nested within the Full model shown in Figure 2.4.








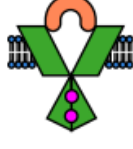
Model	Illustration	Symbol	Definition
All		E	MalE
		M	Maltose
		E_m	Closed, liganded MalE
		A	P-closed transporter (open ATP interface)
		F	P-open E-MalFGK ₂ complex with M associated
Standard		D	Liganded MalE bound to A
Alternate		B	P-open transporter (closed ATP interface)
		C	Unliganded MalE bound to B

Table 2.1: The Comprehensive model consists of all concentration states in the above table.


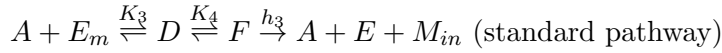
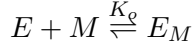
Model	Illustration	Symbol	Definition
Full		G	Unliganded MalE bound to A

Table 2.2: The Full model consists of all concentration states in Table 2.1 and the above table.

2.1 Standard Model

The Standard Model consists of the following reactions:

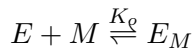


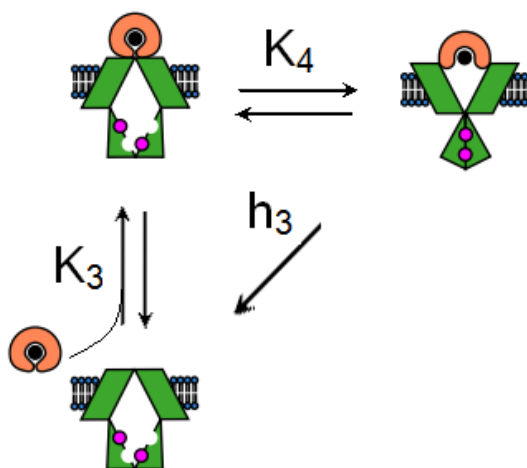
The Standard model includes transporter states A , D , and F as seen in Table 2.2 and Figure 2.1. The single pathway of maltose transport in this model is for a maltose-bound, closed-liganded MalE (E_m) to bind to the closed transporter resting state. This association instigates a conformational change which induces the opening of MalE. Maltose is subsequently released into the binding pocket of the transporter for hydrolysis and import. MalE then dissociates from the transporter and returns to the periplasm. Hydrolysis is assumed to occur at some constant rate h_3 .

MalE-maltose-FGK₂ complex state (F) is the only P-open transporter state in the Standard model. For the sake of comparison to data (discussed later), in the absence of nucleotides we assume the forward rate $k_4^+ = 0$ (see Table 2.4 for kinetic rates), therefore the concentration $F = 0$ in the absence of nucleotides. In the presence of non-hydrolysable AMP-PNP, we assume both P-open states A and D , and P-closed state F are possible.

2.2 Alternate Model

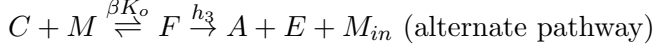
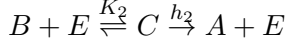
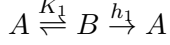
The Alternate model consists of the following reactions:





$E + M \rightleftharpoons E_m$	A	F	D

Figure 2.1: Standard model.



The Alternate model includes MalFGK₂ states A , B , C , and F as shown in Table 2.2 and Figure 2.2. This model does not allow for MalE (liganded or unliganded) to bind to the closed transporter (A), and therefore does not include the standard pathway of maltose transport. The alternate pathway of maltose transport is for an unliganded MalE (E) to bind to the P-open conformation of MalFGK₂ (B), forming a complex (C) which is assumed to be stabilized or increase the affinity of the transporter for maltose. Maltose can then subsequently bind to the complex and be imported to the cytosol via hydrolysis at a rate h_3 . We will refer to this as the alternate pathway of maltose transport.

We also allow for the MalE in complex F to bind maltose, acquire the closed conformation (E_m), and dissociate into the periplasm in an autoregulatory step. We allow this reaction to be reversible such that a maltose-bound MalE can bind to the open transporter (B), and consequently provide an additional pathway of maltose transport. This allows for the investigation of whether maltose-bound MalE may in fact bind to the open transporter in the presence of nucleotides. We refer to this route of maltose transport as the ‘open’ pathway.

ATP hydrolysis is assumed to occur in the absence of MalE and maltose, as shown in nanodisc experiments [1]. In this case the P-open conformation (B) hydrolyzes ATP and returns to the P-closed conformation (A) at a constant rate h_1 . It is also assumed that the MalE-complex C can hydrolyze at a constant rate h_2 , causing the MalE to dissociate and the return of the transporter to the resting state A . Experiments have shown that the addition of MalE to MalFGK₂ increased the ATPase activity 3-fold in nanodiscs and 4-fold in liposomes [1].

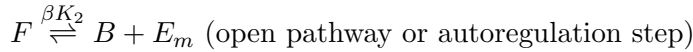
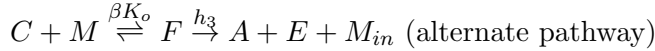
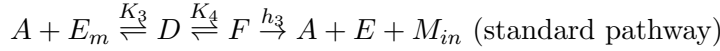
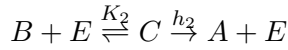
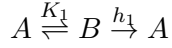
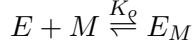
We assume that, in the presence of nucleotides, the forward rate from A to B , k_1^+ , is large compared with the backward rate k_1^- (see Table 2.4 for kinetic rates), therefore the equilibrium constant $K_1 = \frac{k_1^-}{k_1^+} \ll 1$. This assumption is based on experimental evidence that AMP-PNP (non-hydrolysable nucleotides) stabilizes the P-open conformation of MalFGK₂ [1].

The transporter state A is the only P-closed state in the Alternate model. Therefore, in conditions without nucleotides no binding to the transporter can occur for the Alternate model

so we set $k_1^+ = 0$.

2.3 Comprehensive Model

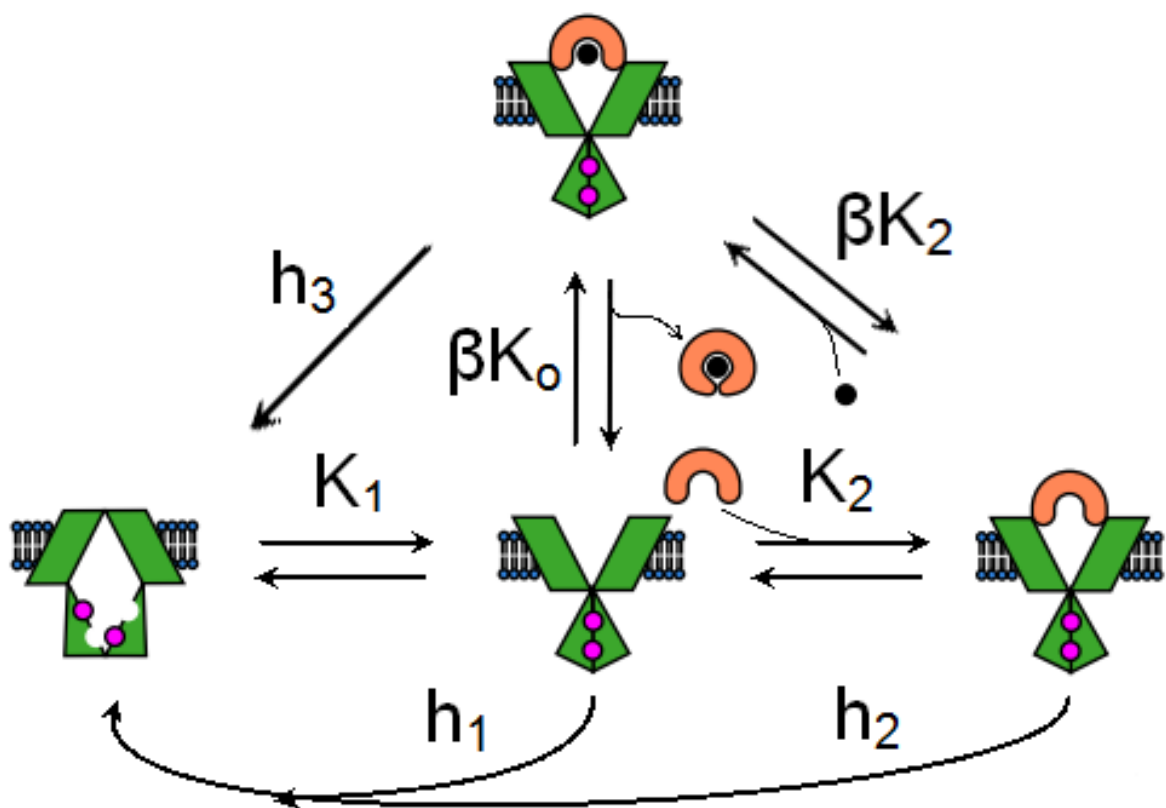
The Comprehensive model consists of the following reactions:



The Comprehensive model combines all reactions from the Standard and Alternate models, and includes transporter states A , B , C , D , and F , as seen in Table 2.2 and Figure 2.3. Equilibrium constants and kinetic rates for the Comprehensive model are found in Table 2.5 and Table 2.4. This model allows for maltose transport to occur through the three pathways described previously and include the standard pathway, the alternate pathway (MalE binds to the open transporter first, maltose binds subsequently), and the open pathway in which E_m binds to the open transporter (B).

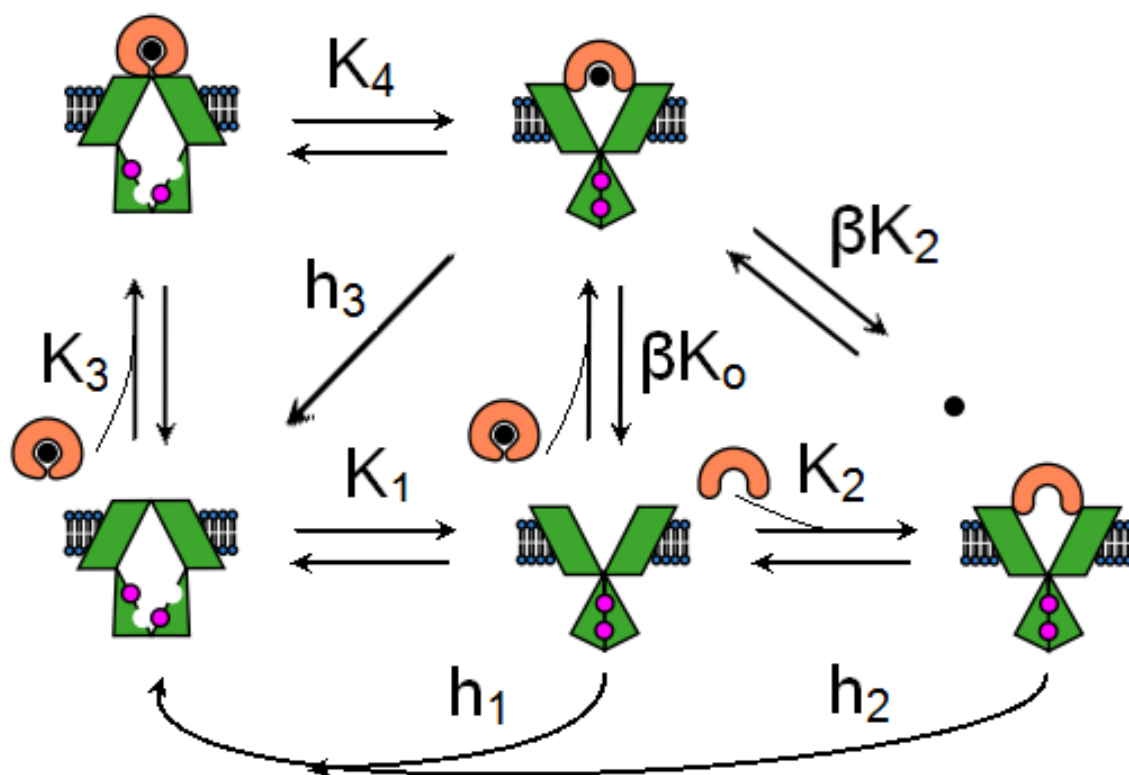
There are three P-open states in the Comprehensive model (B , C , F) which do not occur in the absence of nucleotides. This results from our assumption that the forward rates $k_1^+, k_4^+ = 0$ without nucleotides to close the interface. Therefore $B = C = F = 0$ in conditions without nucleotides.

In the presence of nucleotides, we consider two cases for the Comprehensive model. In the first case, we assume that all transporter states can occur in the presence of non-hydrolysable nucleotides (AMP-PNP) such that the equilibrium parameter K_1 is nonzero. In the second, more simplified case we assume that only P-open transporter states occur in the presence of saturating AMP-PNP, such that $A = D = 0$ in the presence of AMP-PNP (i.e. $K_1 \rightarrow 0$).



$E + M \rightleftharpoons E_m$	A	B	C	F

Figure 2.2: The Alternative model.

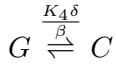
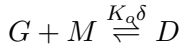
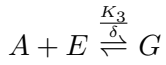
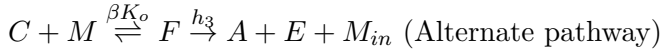
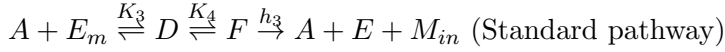
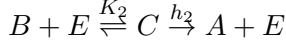
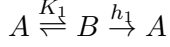
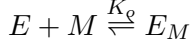


$E + M \rightleftharpoons E_m$	A	B	C	D	F

Figure 2.3: The Comprehensive model.

2.4 Full Model

The Full Model consists of the following reactions:



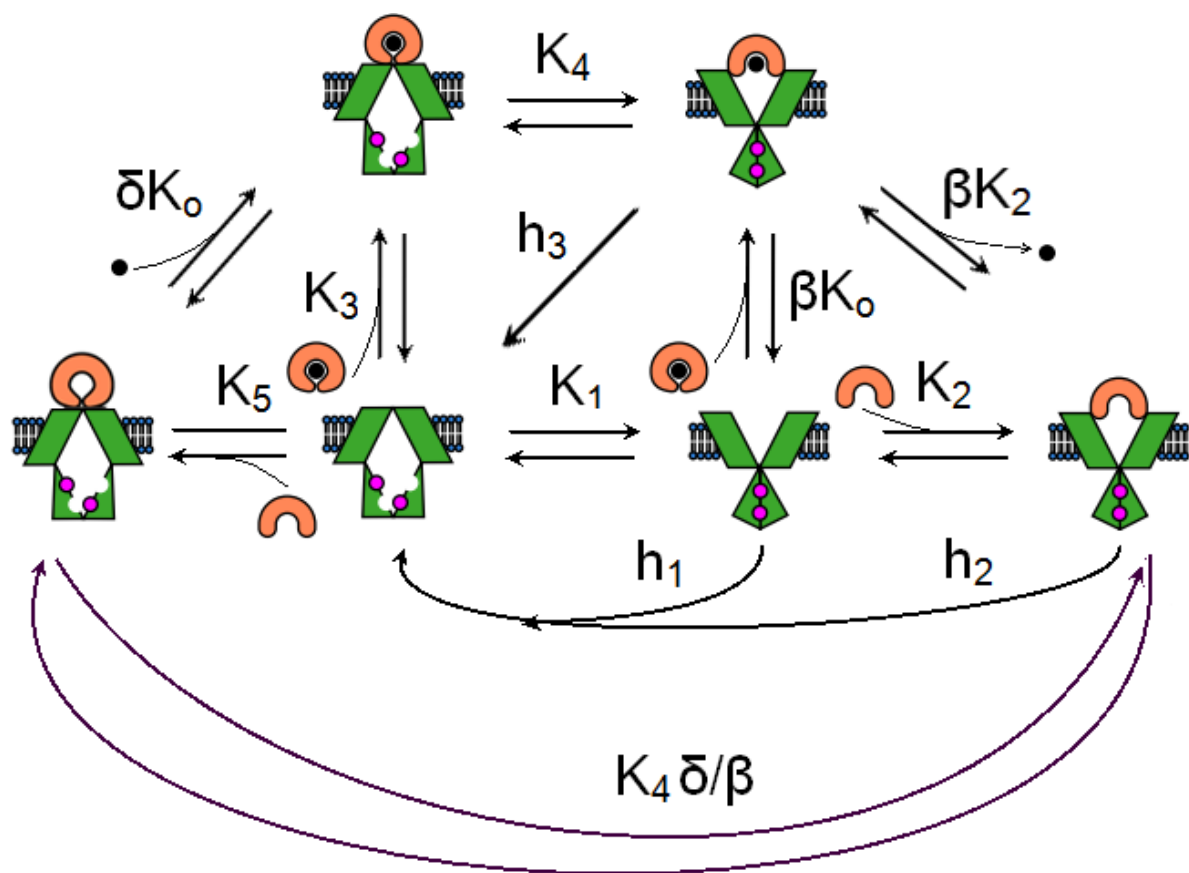
The Full model adds one transporter state (G) and three reversible reactions to the Comprehensive model as seen in Table 2.2 and Figure 2.4. Equilibrium constants and kinetic rates for the Full model are found in Table 2.5 and Table 2.4. The Full model can be diagrammed as a cubed network of reactions. Detailed balance ensures that we only gain one additional equilibrium parameter from the Comprehensive model (δ), in addition to six new kinetic rates for each new forward/reverse reaction, as seen in Table 2.4.

Transporter state G is unliganded MalE bound to P-closed MalFGK₂. This is an unlikely state but equilibrium fluorescence quenching data indicates that there is binding occurring between MalE and MalFGK₂ in the absence of maltose and nucleotides [1], and so we consider state G in order to fit this experimental data.

We allow for unliganded MalE to reversibly bind to the closed transporter and for maltose to subsequently bind to this complex, forming transporter state D (closed transporter in complex with MalE and maltose). The Full model also includes a reversible conformation change between open and closed transporter states with unliganded MalE bound.

In the absence of nucleotides, it is assumed that $B = C = F = 0$ as in the Comprehensive

model. In the presence of AMP-PNP, we consider the stronger assumption that only P-open states occur (at equilibrium). Experimental data were insufficient to fit the larger Full model without this assumption.



$E + M \rightleftharpoons E_m$	A	B	C	D	E	F	G

Figure 2.4: The Full model.

Model	Parameter	Reaction	Units
All	k_o^-	$E + M \leftarrow E_m$	t^{-1}
	k_o^+	$E + M \rightarrow E_m$	$\text{c}^{-1} \text{t}^{-1}$
Standard	k_3^-	$A + E_m \leftarrow D$	t^{-1}
	k_3^+	$A + E_m \rightarrow D$	$\text{c}^{-1} \text{t}^{-1}$
	k_4^-	$D \leftarrow F$	t^{-1}
	k_4^+	$D \rightarrow F$	t^{-1}
Alternate	k_1^-	$A \leftarrow B$	t^{-1}
	k_1^+	$A \rightarrow B$	t^{-1}
	k_2^-	$B + E \leftarrow C$	t^{-1}
	k_2^+	$B + E \rightarrow C$	$\text{c}^{-1} \text{t}^{-1}$
	$\beta_1 k_o^-$	$C + M \leftarrow F$	t^{-1}
	$\beta_o k_o^+$	$C + M \rightarrow F$	$\text{c}^{-1} \text{t}^{-1}$
	$\beta_3 k_2^-$	$B + E_m \leftarrow F$	t^{-1}
	$\beta_2 k_2^+$	$B + E_m \rightarrow F$	$\text{c}^{-1} \text{t}^{-1}$

Table 2.3: The Comprehensive model consists of all of the kinetic rates and reactions in the above table.

Model	Parameter	Reaction	Units
Full	$\delta_1 k_3^+$	$A \rightarrow G$	$\text{c}^{-1}\text{t}^{-1}$
	$\delta_2 k_3^-$	$A \leftarrow G$	t^{-1}
	$\delta_3 k_o^+$	$G \rightarrow D$	$\text{c}^{-1}\text{t}^{-1}$
	$\delta_4 k_o^-$	$G \leftarrow D$	t^{-1}
	$\gamma^+ k_4^+$	$G \rightarrow C$	t^{-1}
	$\gamma^- k_4^-$	$G \leftarrow C$	t^{-1}

Table 2.4: Additional forward and backward kinetic rates for the Full model. The Full model also consists of all parameters and reactions in Table 2.2.

Model	Parameter	Reaction	Units
All	$K_o = \frac{k_o^-}{k_o^+}$	$E + M \xrightleftharpoons{K_o} E_m$	c
Standard	$K_3 = \frac{k_3^-}{k_3^+}$	$A + E_m \xrightleftharpoons{K_3} D$	c
	$K_4 = \frac{k_4^-}{k_4^+}$	$D \xrightleftharpoons{K_4} F$	d
	k_h	$F \xrightarrow{k_h} A + M_{in} + E$	t ⁻¹
Alternate	$K_1 = \frac{k_1^-}{k_1^+}$	$A \xrightleftharpoons{K_1} B$	d
	$K_2 = \frac{k_2^-}{k_2^+}$	$B + E \xrightleftharpoons{K_2} C$	c
	$\beta = \frac{\beta_3}{\beta_2} = \frac{\beta_1}{\beta_o}$	$B + E_m \xrightleftharpoons{\beta K_2} F \xrightleftharpoons{\beta K_o} C + M$	d
	h_1	$B \xrightarrow{h_1} A$	t ⁻¹
	h_2	$C \xrightarrow{h_2} A + E$	t ⁻¹
	h_3	$F \xrightarrow{h_3} A + M_{in} + E$	t ⁻¹
Full	$\delta = \frac{\delta_1}{\delta_2} = \frac{\delta_4}{\delta_3} = \frac{\gamma^- \beta}{\gamma^+}$	$A + E \xrightleftharpoons{\frac{K_3}{\delta}} G + M \xrightleftharpoons{\delta K_o} D, G \xrightleftharpoons{\frac{K_4 \delta}{\beta}} C$	d

Table 2.5: Model parameters with c=concentration, t=time, and d=dimensionless. The Comprehensive model combines all parameters and reactions from the Standard and Alternate models. The Full model consists of all parameters and reactions shown in the above table.

Chapter 3

Experimental Data

Several methods were used to study the maltose uptake system in E.coli, including detergents, liposomes, and nanodiscs [1]. Detergents are used to make membrane proteins soluble by forming detergent-protein-lipid micelles. Detergents have drawbacks for membrane protein stability and can interfere with many molecular techniques, including undesired partitioning of substrates and products [13]. Liposomes are most useful when compartmentalization of each side of the bilayer is needed [13]. However, liposomes are large, unstable, and difficult to prepare with precisely controlled size and stoichiometry.

Because of the drawbacks associated with detergents and liposomes, nanodiscs are used as an alternative technique for studying membrane proteins. Nanodiscs are soluble nanoscale phospholipid bilayers which have been used to study the MalFGK₂ transporter [1]. Nanodiscs can self-assemble integral membrane proteins and are therefore useful for understanding membrane protein function [13]. Nanodiscs allow for solubility of membrane proteins at the single molecule level. This is advantageous compared with liposomes or detergent micelles in terms of the size, stability, and access to both sides of the phospholipid bilayer domain. It also offers advantages in adding genetically modifiable features to the Nanodisc structure [13].

Fluorescence Quenching, specifically an electron-transfer based quenching reaction, was used as a measure of binding between MalFGK₂ in nanodiscs (Nd-FGK₂) and MalE. Quenching was measured at constant MalE concentration, with increasing concentration of Nd-FGK₂ in the presence or absence of nucleotides and in the presence or absence of maltose. In the case where nucleotides were present, AMP-PNP was used as a non-hydrolysable ATP analog. This condition stabilizes the P-open state transporter [1].

The ATPase activity was measured at 37° C using Nd-FGK₂ in the presence of ATP, in the presence or absence of MalE, and in the presence or absence of maltose [1]. The basal ATPase activity in the nanodisc was found to be approximately 10 fold higher than in proteoliposomes, however in both cases MalE increased the rate of ATP hydrolysis. There was a 3-fold increase in nanodiscs and a 4-fold increase in proteoliposomes. In the presence of maltose, an inhibition of the ATPase activity was observed in nanodiscs which was not observed in proteoliposomes. It was proposed that maltose could negatively affect the association of MalE with the transporter [1].

3.1 Fluorescence Quenching Experiments

All experimental data used for this analysis comes from experiments with MalFGK₂ in nanodiscs. We will refer to MalFGK₂ in nanodiscs as Nd-FGK₂. Fluorescence Quenching, specifically an electron-transfer based quenching reaction, was used as a measure of binding between MalFGK₂ in nanodiscs (Nd-FGK₂) and MalE. Equilibrium quenching was measured for a fixed MalE concentration, for a range of increasing concentration of Nd-FGK₂ in the presence or absence of nucleotides and in the presence or absence of maltose. In the case where nucleotides were present, AMP-PNP was used as a non-hydrolysable ATP analog. This condition stabilizes the P-open state transporter [1].

3.2 Equilibrium Data

The equilibrium quenching was measured as a function of increasing Nd-FGK₂ concentration for a fixed total MalE concentration of 20 nM. Experiments were done in the presence or absence of 1 mM of maltose, as shown in Figure 3.1.

3.3 Time-Dependent Data

Fluorescence quenching was measured as a function of time in minutes. The concentration of MalFGK₂ was fixed at 90 nM, and the concentration of MalE at 20nM. We consider the experiment performed in the presence of AMP-PNP and in the absence of maltose as seen in Figure 3.2.

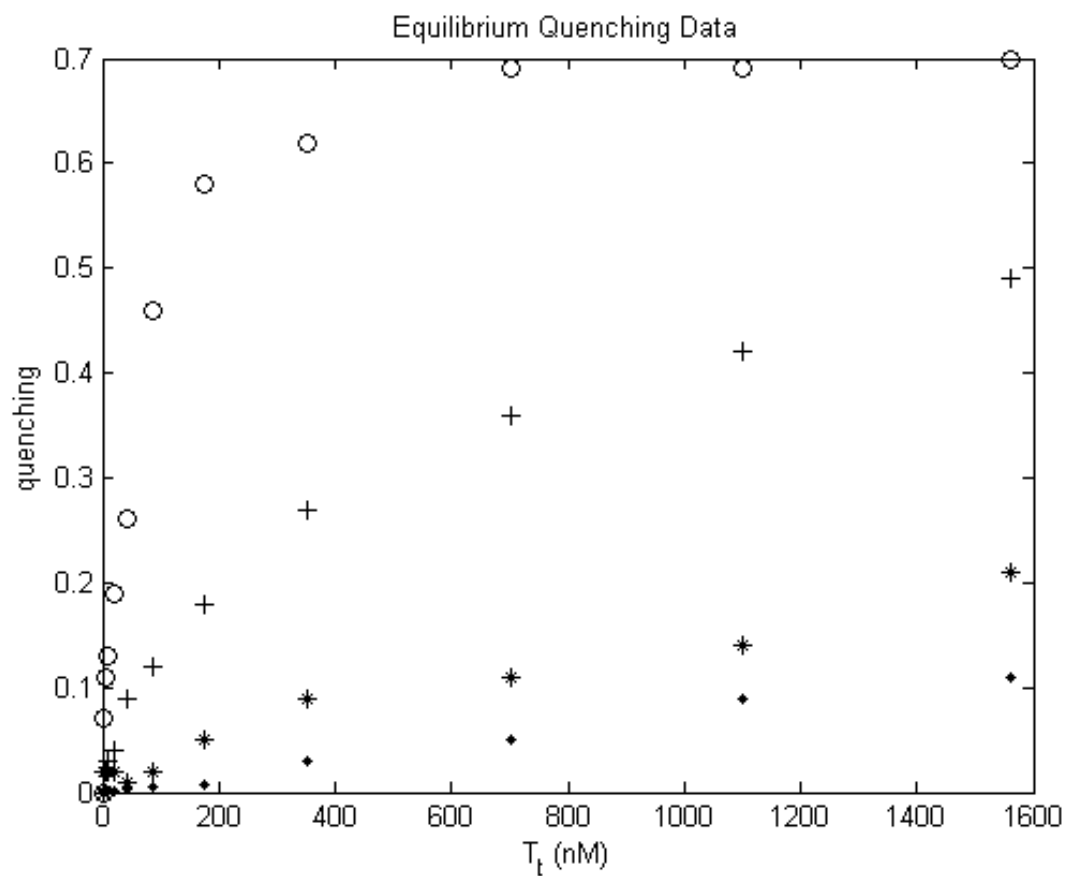


Figure 3.1: Equilibrium quenching data under 4 conditions: o= AMP-PNP (no maltose), + = AMP-PNP (with maltose), *=no nucleotides (no maltose), ·=no nucleotides (with maltose). T_t is total concentration of Nd-FGK₂. This data appears in [1].

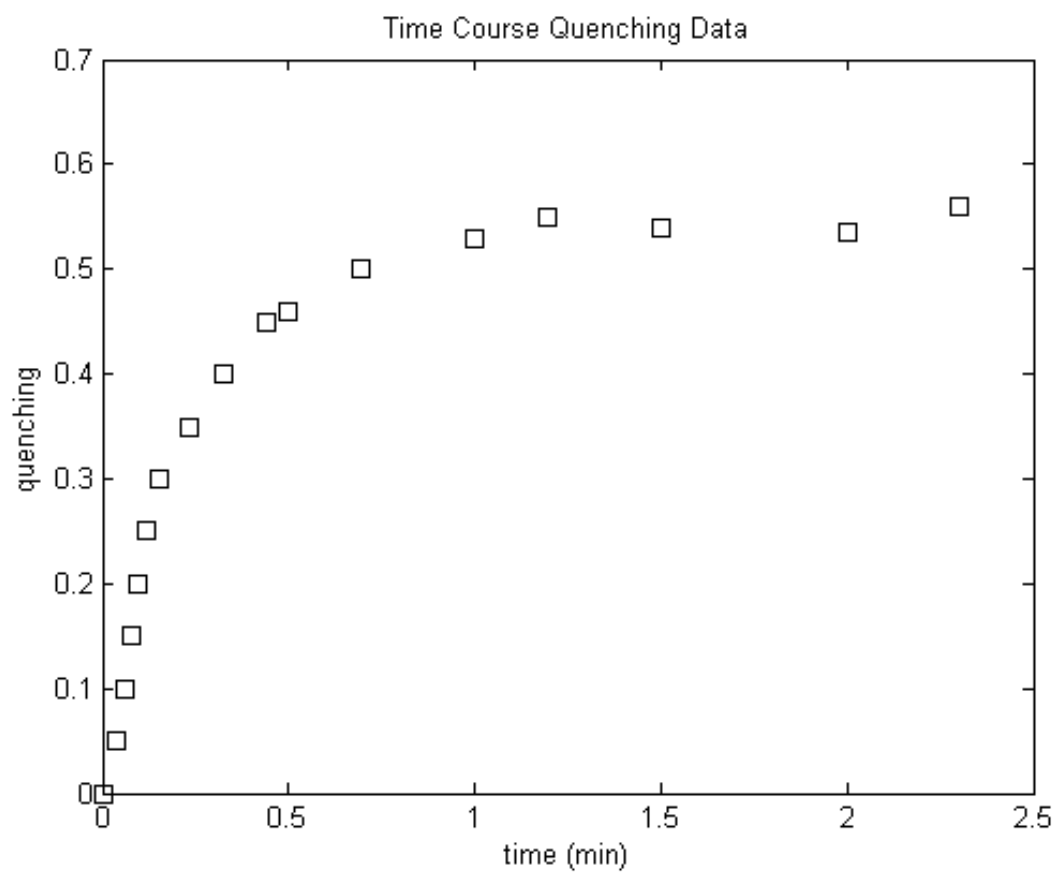


Figure 3.2: Time course quenching data in the presence of AMP-PNP to block hydrolysis, Male (20 nM), and Nd-FGK₂ (90 nM).

3.4 ATPase Experiments

Steady-state ATPase rates were measured for concentrations of MalE and Nd-FGK₂ fixed at 2 μ M in the presence of ATP. Experiments were performed under three conditions in nanodiscs: in the presence of MalE and maltose, in the presence of MalE only, and with only Nd-FGK₂.

3.5 Fit Methods

All models were fit to equilibrium fluorescence quenching data measured under hydrolysis-blocking conditions, as well as to the steady-state ATPase data. The time-dependent data measured in the absence of maltose was used to fit the kinetic rate k_2^+ in the Comprehensive model, as well as to estimate the magnitude of the rate k_1^+ , the forward rate of the conformation change from P-closed to P-open transporter.

Nonlinear regression and Matlab[®] were used to fit model parameters to experimental data and to generate confidence intervals on fit values. Estimates of equilibrium constants and hydrolysis rates of the maltose uptake system in nanodiscs were obtained for each model. Equilibrium fluorescence quenching data for Nd-FGK₂ and MalE were used fit the equilibrium constants ($K_i = \frac{k_i^-}{k_i^+}$). ATPase data were used to solve for the hydrolysis rates h_1 , h_2 , h_3 , using fit equilibrium values.

We assume that hydrolysis is the rate limiting step, and that we are at equilibrium under hydrolysis-blocking conditions. At equilibrium, the concentrations of each transporter state are found explicitly as a function of maltose, K_o (the affinity of MalE for maltose), and all other relevant equilibrium constants.

To fit the quenching data we assume that in each model, the transporter states that have MalE bound represent quenching concentrations. We assume that the quenching data has been vertically scaled by some common unknown constant ϕ , which was fit in addition to all model parameters.

3.6 Fit Analysis

The Standard model and Alternate model have the same number of equilibrium constants being fit to the data. Both models are fit to three data sets (n=36), under conditions with AMP-

PNP (with and without maltose) and in the absence of nucleotides with maltose present. The sum of the squared residual error (SSR) is compared to determine which model is a better fit to the equilibrium data set. Neither the Standard or Alternate models have binding between MalE and MalFGK₂ under conditions without nucleotides and without maltose, so this experimental data set is omitted from this comparison for simplicity.

The Standard and Alternate model are both nested within the Comprehensive model. An F-test was used to determine whether the Comprehensive model is a significantly better fit to the three equilibrium data sets than the Standard or Alternate models. The Comprehensive model also has no fit to experimental data in the absence of both nucleotides and maltose, allowing for comparison of the Standard, Alternate, and Comprehensive models using only the three data sets described.

In order to fit the fourth experimental equilibrium data set measured in the absence of both nucleotides and maltose, the Comprehensive and Full models are both fit to all four equilibrium data sets (n=48). The function quenching=0 was used for the Comprehensive model in the fourth data set in order to compare fits with the Full model. The Comprehensive model is nested within the Full model, and an F-test is used to determine whether the additional parameter in the Full model produces a significantly better fit to the four data sets. We consider in this case whether the extra data set measured in the absence of nucleotides and maltose is significant to the overall maltose uptake system.

Chapter 4

Nonlinear Regression Fit

4.1 Equilibrium Data Fit

4.1.1 Standard Model

In the absense of hydrolysis we have the following equalities at equilibrium for the standard model:

$$D = \frac{AE_m}{K_3}, F = \frac{D}{K_4}, E = \frac{E_m K_o}{M},$$

$$A + D + F = T_t,$$

$$E + D + F + E_m = E_t,$$

where T_t =total [NdFGK₂], E_t =total [MalE].

From this system we obtain the following equilibrium concentration functions for each state:

$$D = 0.5\left(\left(\frac{E_t}{\omega} + \frac{T_t}{\omega} + \frac{K_3\gamma}{\omega^2}\right) \pm \sqrt{\left(\frac{E_t}{\omega} + \frac{T_t}{\omega} + \frac{K_3\gamma}{\omega^2}\right)^2 - 4\frac{T_t E_t}{\omega^2}}\right)$$

$$\text{where } \gamma = \frac{K_o}{M} + 1, \omega = 1 + \frac{1}{K_4},$$

$$F = \frac{D}{K_4},$$

$$A = T_t - D - F,$$

$$E_m = \frac{E_o - \omega D}{\gamma}, \text{ and}$$

$$E = \frac{E_m K_o}{M}.$$

See Appendix A for full derivation and nondimensionalization. The nondimensional equations were fit to equilibrium quenching data for experiments for comparison to the CS model. Each data set contains twelve measurements (n=36). The data were measured under the following conditions: 1) no nucleotides with maltose, 2) AMP-PNP with maltose, and 3) AMP-PNP without maltose. The nondimensionalized versions of the functions below were used to fit each data set:

1. quenching = $\frac{D}{\phi}$,
2. quenching = $\frac{D+F}{\phi}$,
3. quenching = 0 was used for comparison to Alternate model fit, as no binding occurs between MalFGK₂ and MalE for the Standard model.

The Standard model was fit for the equilibrium constants K_3 and K_4 , and the vertical scaling constant ϕ . Fit results are shown in Table 4.1 and in Figure 4.1.

4.1.2 Alternate Model

In the absense of hydrolysis we have the following equalities at equilibrium for the Alternate model:

$$A = K_1 B,$$

$$BE = K_2 C,$$

$$BE_m = \beta K_2 F,$$

$$\beta K_o F = CM,$$

$$EM = K_o E_m,$$

$$A + B + C + F = T_t, \text{ and}$$

$$E + E_m + C + F = E_t.$$

From this system we obtain the following equilibrium functions for concentration of each state:

$$C = 0.5[(\frac{\psi\xi}{\nu^2} + \frac{E_t}{\nu} + \frac{T_t}{\nu}) \pm \sqrt{(\frac{\psi\xi}{\nu^2} + \frac{E_t}{\nu} + \frac{T_t}{\nu})^2 - \frac{4T_tE_t}{\nu^2}}]$$

where $\psi = K_2(K_1 + 1)$, $\xi = 1 + \frac{M}{K_o}$, $\nu = 1 + \sigma$, and $\sigma = \frac{M}{K_o\beta}$. All other variables can be expressed in terms of C as follows:

$$E = \frac{E_t - \nu C}{\xi} ,$$

$$E_m = \frac{EM}{K_o} ,$$

$$B = K_2 C \frac{\xi}{E_t - \nu C} ,$$

$$A = K_1 B , \text{ and}$$

$$F = \sigma C .$$

See Appendix B for full derivation and nondimensionalization. The nondimensional equations were fit to equilibrium quenching data for the same three experiments for comparison to the Standard model and Comprehensive model. Each data set contains twelve measurements (n=36). The data were measured under the following conditions: 1) no nucleotides with maltose, 2) AMP-PNP with maltose, and 3) AMP-PNP without maltose. The nondimensionalized versions of the functions below were used to fit each data set:

1. quenching = 0 was used for comparison to the Standard model fit as no binding occurs between MalFGK₂ and MalE for the Alternate model ,
2. quenching = $\frac{C+F}{\phi}$,
3. quenching = $\frac{C}{\phi}$.

The Alternate model was fit for equilibrium parameters K_2 and β , using the assumption that $K_1 \ll 1$ in the presence of AMP-PNP, so that $\psi = K_2$. We do this to eliminate the need to fit K_1 []. Evidence for this assumption comes from experiments indicating that the P-open conformation of the transporter is stabilized in the presence of non-hydrolyzable nucleotides [1]. Stabilized P-open transporters would correspond to $k_1^- \ll 1$, where k_1 is the backward rate from the P-open to P-closed transporter states: $A \leftarrow B$, and $K_1 = \frac{k_1^-}{k_1^+}$. See Table 4.1 and Figure 4.1 for fit results.

Model	Parameter	Fit Value	95% Confidence Interval
Standard	K_3	$6.509832 \mu M$	$(-24.37, 37.39) \mu M$
	K_4	0.059	$(-0.2696, 0.3877)$
	ϕ	34.7222	$(-20.123, 89.5674)$
	k_h	0.7514 min^{-1}	
Alternate	K_2	44.94 nM	$(30.702, 59.176) \text{ nM}$
	β	14.3858	$(9.7109, 19.0607)$
	ϕ	27.943	$(26.2673, 29.6188)$
	h_1	0.35 min^{-1}	
	h_2	1.2212 min^{-1}	$(1.2034, 1.2371) \text{ min}^{-1}$
	h_3	0.9575 min^{-1}	$(0.8767, 1.0492) \text{ min}^{-1}$

Table 4.1: Fit values for Standard and Alternate models. Hydrolysis rates were calculated using experimental values found in [1] and fit values above. The value of h_1 has no dependence on fit values and therefore does not have a confidence interval.

4.1.3 Comprehensive Model

In the absense of hydrolysis we have the following equalities at equilibrium for the Comprehensive model:

$$A = K_1 B,$$

$$BE = K_2 C,$$

$$BE_m = \beta K_2 F,$$

$$\beta K_o F = CM,$$

$$D = K_4 F,$$

$$E + E_m + C + D + F = E_t, \text{ and}$$

$$A + B + C + D + F = T_t.$$

From this system we obtain the following equilibrium functions for concentration of each state:

$$C = 0.5[(\frac{\psi\xi}{\alpha^2} + \frac{E_o}{\alpha} + \frac{T_o}{\alpha}) \pm \sqrt{(\frac{\psi\xi}{\alpha^2} + \frac{E_o}{\alpha} + \frac{T_o}{\alpha})^2 - \frac{4T_o E_o}{\alpha^2}}]$$

where $\sigma = \frac{M}{K_o\beta}$, $\xi = 1 + \frac{M}{K_o}$, $\alpha = 1 + \sigma(K_4 + 1)$, and $\psi = K_2(1 + K_1)$. All other variables can be expressed in terms of C as follows:

$$F = \sigma C,$$

$$D = K_4 F,$$

$$E_m = \frac{EM}{K_o},$$

$$E = \frac{E_o - \alpha C}{\xi}, \text{ and}$$

$$B = \frac{K_2 C \xi}{E_o - \alpha C}.$$

See Appendix for full derivation and nondimensionalization. The nondimensional equations were fit to the same equilibrium quenching data for three experiments for comparison to the Alternate model. Each data set contains twelve measurements (n=36). The data were measured under the following conditions: 1) no nucleotides with maltose, 2) AMP-PNP with maltose, and 3) AMP-PNP without maltose. The nondimensionalized versions of the functions below were

used to fit each data set:

1. quenching= $\frac{D}{\phi}$,
2. quenching= $\frac{C+D+F}{\phi}$,
3. quenching= $\frac{C}{\phi}$.

The Comprehensive model was fit for equilibrium parameters K_2 , K_3 , and β and scaling constant ϕ . To allow for the possibility that K_1 is not very small in the presense of nucleotides, and to determine the effect of the magnitude of K_1 on model fits, the value of K_1 was fixed at 0.01, 0.1, 1, and 100. The value of K_4 was calculated using detailed balance. See Table ??, Table ??, and Figure 4.1 for fit results. We also fit equilibrium constants in the Comprehensive model using the simpler assumption that $K_1 \rightarrow 0$ in the presense of AMP-PNP (the ATP interface closes and is stabilized for all transporter present). See Appendix C for full derivation, and Table 4.6 for fit results.

4.1.4 Full Model

The concentrations of each state in the Full model at equilibrium were found using the following equalities and conservation equations:

$$A = K_1 B,$$

$$BE = K_2 C,$$

$$BE_m = \beta K_2 F,$$

$$\beta K_o F = CM,$$

$$D = K_4 F,$$

$$AE = \frac{K_3}{\delta} G,$$

$$AE_m = K_3 D,$$

$$E + E_m + C + D + F + G = E_t,$$

$$A + B + C + D + F + G = T_t,$$

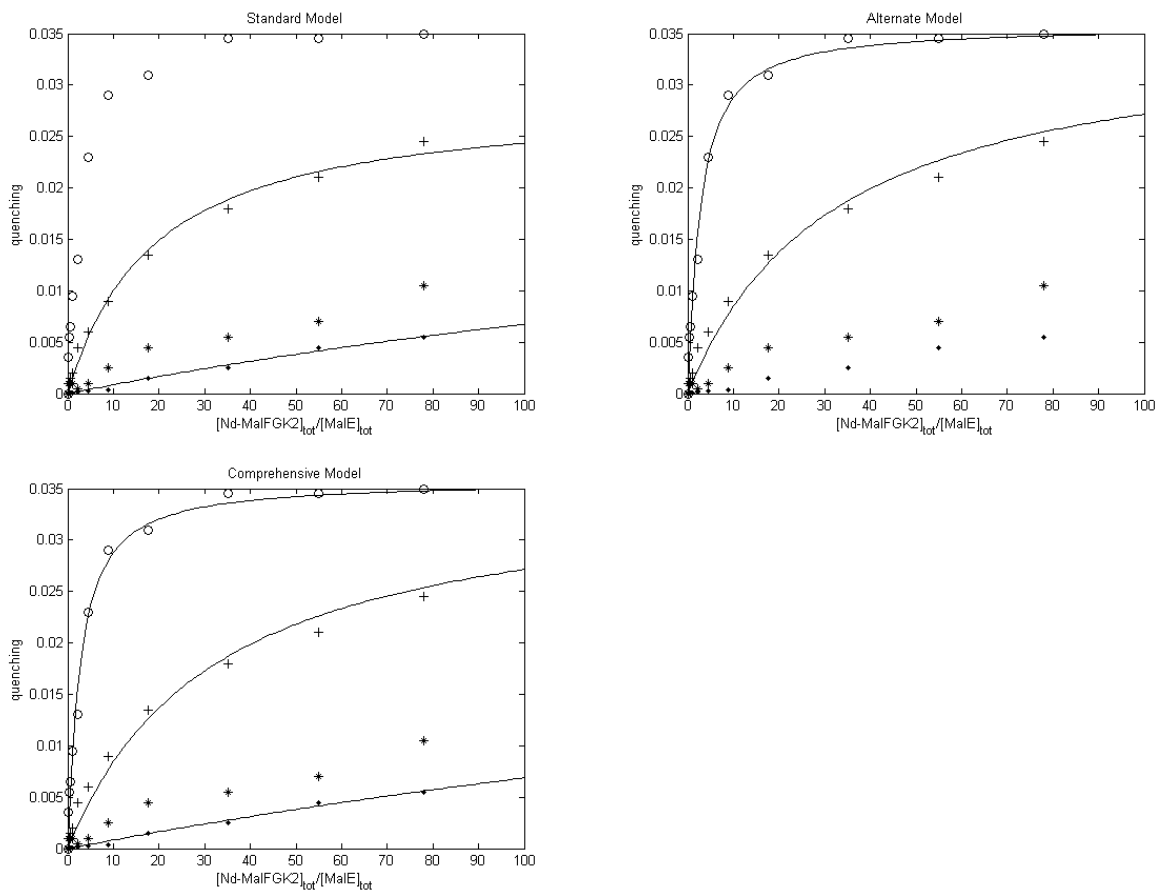


Figure 4.1: Equilibrium quenching data under 4 conditions: \circ = AMP-PNP (no maltose), $+$ = AMP-PNP (with maltose), $*$ =no nucleotides (no maltose), \cdot =no nucleotides (with maltose). The Standard model (upper left) has no fit to data in the absence of maltose. The Alternate model (upper right) has no fit in the absence of nucleotides. The Comprehensive model (lower) has no fit under conditions of no nucleotides when maltose is absent but does fit the data when maltose is present.

K_1	Parameter	Fit Value	95% Confidence Interval
0.01	β	14.3966	(11.3702, 17.4231)
	K_2	44.49703 nM	(35.3802, 53.61188) nM
	K_4	0.00076413	(0.0005, 0.001)
	K_3	8.3833 μM	(5.4992, 11.2673) μM
	ϕ	27.9428	(26.859, 29.0265)
	h_1	0.3535 min ⁻¹	
	h_2	1.2212 min ⁻¹	(1.2072, 1.234) min ⁻¹
	h_3	0.9583 min ⁻¹	(0.8927, 1.0306) min ⁻¹

Table 4.2: Fit to nanodisc data for Comprehensive model parameters, for $K_1 = 0.01$. Hydrolysis rates were calculated using experimental values found in [1] and fit values above. The value of h_1 has no dependence on fit values and therefore does not have a confidence interval.

K_1	Parameter	Fit Value	95% Confidence Interval
0.1	β	14.4872	(11.4347, 17.5397)
	K_2	40.85636 nM	(32.48545, 49.22545) nM
	K_4	0.0071	(0.0044, 0.0097)
	K_3	8.3833 μM	(5.4992, 11.2673) μM
	ϕ	27.9428	(26.859, 29.0265)
	h_1	0.3535 min ⁻¹	
	h_2	1.2212 min ⁻¹	(1.2072, 1.234) min ⁻¹
	h_3	0.9643 min ⁻¹	(0.8964, 1.0392) min ⁻¹

Table 4.3: Fit to nanodisc data for Comprehensive model parameters, for $K_1 = 0.1$. Hydrolysis rates were calculated using experimental values found in [1] and fit values above. The value of h_1 has no dependence on fit values and therefore does not have a confidence interval.

K_1	Parameter	Fit Value	95% Confidence Interval
1	β	14.9625	(11.766, 18.159)
	K_2	22.471 nM	(17.867, 27.074) nM
	K_4	0.0401	(0.0248, 0.0554)
	K_3	8.3833 μM	(5.4992, 11.2673) μM
	ϕ	27.9428	(26.859, 29.0265)
	h_1	0.7 min ⁻¹	
	h_2	1.2212 min ⁻¹	(1.2072, 1.234) min ⁻¹
	h_3	0.9959 min ⁻¹	0.9156, 1.084) min ⁻¹

Table 4.4: Fit to nanodisc data for Comprehensive model parameters, for $K_1 = 1$. Hydrolysis rates were calculated using experimental values found in [1] and fit values above. The value of h_1 has no dependence on fit values and therefore does not have a confidence interval.

100	β	14.9625	(11.766, 18.159)
	K_2	0.44497 nM	(0.353802, 0.536119) nM
	K_4	0.0827	(0.0498, 0.1156)
	K_3	8.3833 μM	(5.4992, 11.2673) μM
	ϕ	27.9428	(26.859, 29.0265)
	h_1	35.35 min ⁻¹	
	h_2	1.2212 min ⁻¹	(1.2072, 1.234) min ⁻¹
	h_3	1.0367 min ⁻¹	(0.9392, 1.1431) min ⁻¹

Table 4.5: Fit to nanodisc data for Comprehensive model parameters, for $K_1 = 100$. Hydrolysis rates were calculated using experimental values found in [1] and fit values above. The value of h_1 has no dependence on fit values and therefore does not have a confidence interval.

K_1	Parameter	Fit Value	95% Confidence Interval
All Values	β	14.3856	(11.3623, 17.4089)
	K_2	44.942 nM	(35.734, 54.148) nM
	K_3	8.3833 μM	(5.4992, 11.2673) μM
	ϕ	27.9428	(26.859, 29.0265)

Table 4.6: Fit to Comprehensive model with the assumption that $K_1 \rightarrow 0$. The parameter $K_4 = \frac{\beta K_2 K_1}{K_3}$ using detailed balance. The hydrolysis rate h_1 is also a function of K_1 as shown in Section 4.3. As $K_1 \rightarrow 0$, $h_1 \rightarrow 0.35$ min⁻¹.

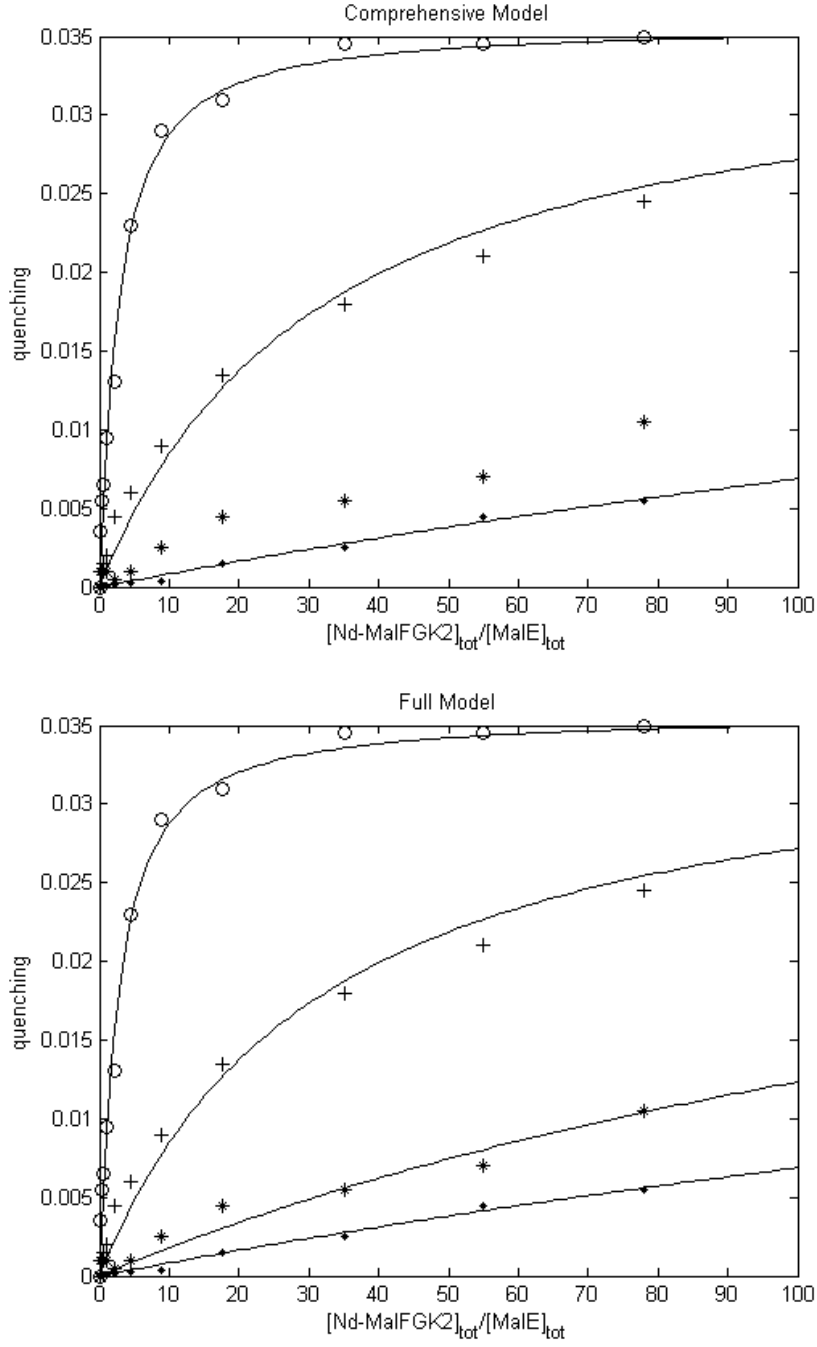


Figure 4.2: Equilibrium fit for Comprehensive model (top) and Full model (bottom). Equilibrium quenching data under 4 conditions: o= AMP-PNP (no maltose), + = AMP-PNP (with maltose), *=no nucleotides (no maltose), ·=no nucleotides (with maltose).

$F = \sigma C$, where $\sigma = \frac{M}{K_o\beta}$ and

$$E_m = \frac{EM}{K_o}.$$

We assume that in the absense of nucleotides, we only have P-closed transporter states:

$$A + D + G = T_t,$$

$$E + E_m + D + G = E_t.$$

Then,

$$G = 0.5\left[\left(\frac{K_3\gamma}{\xi^2\delta} + \frac{E_t}{\xi} + \frac{T_t}{\xi}\right) \pm \sqrt{\left(\frac{K_3\gamma}{\xi^2\delta} + \frac{E_t}{\xi} + \frac{T_t}{\xi}\right)^2 - \frac{4T_tE_t}{\xi^2}}\right], \text{ and}$$

$$D = \frac{M}{K_o\delta}G, \text{ where } \xi = 1 + \frac{M}{K_o\delta}.$$

See Appendix for full derivation and nondimensionalization. The nondimensional equations were fit to the equilibrium quenching data for all four experimental conditions for comparison to the Alternate model. Each data set contains twelve measurements (n=48). The data were measured under the following conditions: 1) no nucleotides with maltose, 2) AMP-PNP with maltose, 3) AMP-PNP without maltose, and 4) no nucleotides without maltose. The nondimensionalized versions of the functions below were used to fit each data set:

1. quenching = $\frac{D+G}{\phi}$,
2. quenching = $\frac{C+F}{\phi}$,
3. quenching = $\frac{C}{\phi}$,
4. quenching = $\frac{G}{\phi}$.

The Full model was fit for equilibrium parameters K_2 , K_3 , β , δ , and scaling constant ϕ . Experimental data were insufficient to fit K_1 , therefore the value of K_1 was fixed at 0.01 and the value of K_4 was calculated using detailed balance. See Table 4.7 and Figure 4.2 for fit results.

Parameter	Fit Value $ _{K_1=0.01}$	95% Confidence Interval
β	14.3914	(11.5781, 17.2046)
δ	2.2197	(1.3961, 3.0433)
K_2	44.888 nM	(36.334, 53.44) nM
K_4	0.000767477	(0.0005, 0.001)
K_3	8.417206 μM	(5.713, 11.12141) μM
$K_5 = \frac{K_3}{\delta}$	0.000118374	(0.0000887903, 0.00146) μM
ϕ	27.9523	(26.9445, 28.9601)

Table 4.7: Fit to Full model parameters. Here K_4 again depends on K_1 using detailed balance, and h_1 depends on K_1 .

4.2 Time-Dependent Data Fit

4.2.1 In the limit $K_1 \rightarrow 0$

If we assume that AMP-PNP closes and stabilizes the ATP interface for all transporters present ($K_1 \rightarrow 0$), we can fit the value of k_2^+ using experimental time course of the quenching data in the presence of AMP-PNP (no maltose). The result relies upon our fit value of $K_2 = 44.942$ nM, where K_2 was also fit under the assumption that $K_1 \rightarrow 0$. In the absence of maltose and of P-closed MalFGK₂, we have the following system of ordinary differential equations

$$B + C = T_t,$$

$$C + E = E_t,$$

$$\frac{dB}{dt} = -k_2^+ BE + k_2^- C$$

$$\frac{dC}{dt} = k_2^+ BE - k_2^- C$$

$$\frac{dE}{dt} = -k_2^+ BE + k_2^- C$$

which can be simplified to give:

$$\frac{dC}{dt} = k_2^+(T_t - C)(E_t - C) - k_2^- C$$

$$C(t) = \frac{c^+(1 - e^{bk_2^+ t})}{1 - \frac{c^+}{c^-} e^{bk_2^+ t}},$$

where, using $E_t = 20$ nM, $T_t = 90$ nM:

$$b = \sqrt{(110 + K_2)^2 - 7200}$$

$$c^+ = \frac{110 + K_2 + b}{2}$$

$$c^- = \frac{110 + K_2 - b}{2}.$$

The fit to time course data gives $k_2^+ = 0.0324 \text{ (nm)}^{-1}(\text{min})^{-1}$, with 95% confidence interval (0.0289, 0.0359) and sum of squared residual error (SSR) 0.0055, using $K_2 = 44.942$ nM. See Figure 4.3 for fit to time course data.

4.2.2 Fixed K_1 , k_1^+

We now consider the less simplified case where both P-open and P-closed transporters can occur in the presence of AMP-PNP ($K_1 \neq 0$). In the absence of maltose, and in the presence of AMP-PNP to block hydrolysis, we have the following system of ordinary differential equations for the Comprehensive model:

$$\frac{dA}{dt} = -k_1^+ A + k_1^- B$$

$$\frac{dB}{dt} = k_1^+ A - k_1^- B - k_2^+ BE + k_2^- C$$

$$\frac{dC}{dt} = -k_2^- C + k_2^+ BE$$

$$A + B + C = T_t$$

$$C + E = E_t$$

Substituting $A = T_t - B - C$, and $E = E_t - C$ into the above system, we obtain:

$$\frac{dB}{dt} = k_1^+(T_t - B - C) - k_1^- B - k_2^+ B(E_t - C) + k_2^- C$$

$$\frac{dC}{dt} = -k_2^- C + k_2^+ B(E_t - C).$$

We let b , c , and τ be nondimensional variables such that $b = \frac{B}{E_t}$, $c = \frac{C}{E_t}$, $\tau = tk_1^+$, $\kappa = \frac{k_2^+}{k_1^+}$, $\kappa_1 = K_2\kappa$, $\kappa_2 = \kappa E_t$:

$$\frac{db}{d\tau} = (\rho - b - c) - K_1 b - \kappa_2 b(1 - c) + \kappa_1 c$$

$$\frac{dc}{d\tau} = -\kappa_1 c + \kappa_2 b(1 - c)$$

We fit k_2^+ for a fixed magnitude of k_1^+ and K_1 , and fit value $K_2 = 44.49703$ nM. See Figure 4.3 and Table 4.8 for fit results. It was necessary to fix both k_1^+ and K_1 rather than allowing the regression to fit the best values, as the one time-dependent quenching data set was only sufficient to fit k_2^+ and the quenching vertical scaling constant ϕ . For each fixed K_1 , we observed how the magnitude of k_1^+ changes the fit value of k_2^+ and the associated SSR for the fit.

4.3 ATPase Data Fit

To calculate the hydrolysis rates in each model, the following functions were used where B, C, F are as written above.

$$h_1 B|_{E_t=0, M=0} = R_1$$

$$h_1 B|_{M=0} + h_2 C|_{M=0} = R_2$$

$$h_1 B + h_2 C + h_3 F = R_3$$

where $R_{1,2,3}$ are the experimental NdFGK₂ ATPase rates measured in the presense of 1) No MalE and no maltose, 2) MalE without maltose, 3) MalE and maltose. Fit values of equilibrium parameters were used to calculate hydrolysis rates and their confidence intervals for each model.

K_1	$k_1^+ \text{ min}^{-1}$ (fixed)	$k_2^+ \text{ nm}^{-1} \text{ min}^{-1}$ (fit)	SSR
0.01	1	1.983	$2.1638 * 10^{-4}$
	10	0.0927	$5.1046 * 10^{-5}$
	10^2	0.0356	$1.2705 * 10^{-5}$
	10^3	0.0327	$1.3475 * 10^{-5}$
	10^4	0.0324	$1.367 * 10^{-5}$
0.1	1	3.6924	$1.8126 * 10^{-4}$
	10	0.0932	$4.9812 * 10^{-5}$
	10^2	0.0385	$1.2669 * 10^{-5}$
	10^3	0.0356	$1.3492 * 10^{-5}$
	10^4	0.0353	$1.3672 * 10^{-5}$
1	1	3.2416	$6.057 * 10^{-5}$
	10	0.1110	$3.3526 * 10^{-5}$
	10^2	0.0674	$1.2850 * 10^{-5}$
	10^3	0.0645	$1.3581 * 10^{-5}$
	10^4	0.0642	$1.3681 * 10^{-5}$
100	1	7.4885	$2.0009 * 10^{-5}$
	10	3.4511	$1.3791 * 10^{-5}$
	10^2	3.2609	$1.3695 * 10^{-5}$
	10^3	3.2429	$1.3693 * 10^{-5}$
	10^4	3.4686	$1.422 * 10^{-5}$

Table 4.8: Fit of k_2^+ for fixed K_1 , k_1^+ . Values of $k_1^+ < 1$ gave fits to the data with higher SSR than for $k_1^+ > 1$. Best fits to the data occurred for $k_1^+ = 10^2 \text{ min}^{-1}$. Furthermore, the best fit occurred for $K_1 = 0.1$, $k_1^+ = 10^2 \text{ min}^{-1}$, $k_2^+ = 0.0385 \text{ nm}^{-1} \text{ min}^{-1}$.

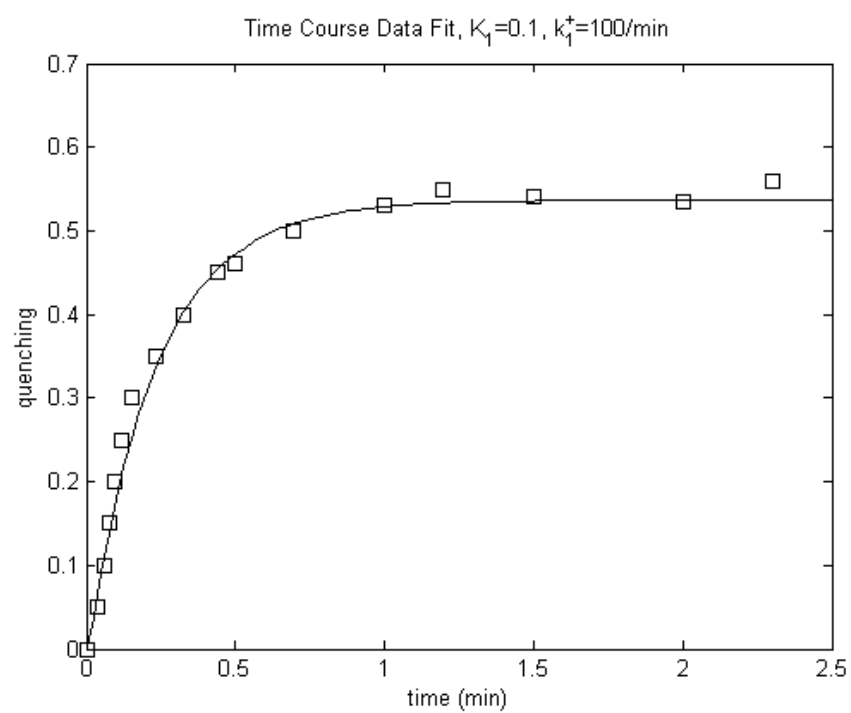
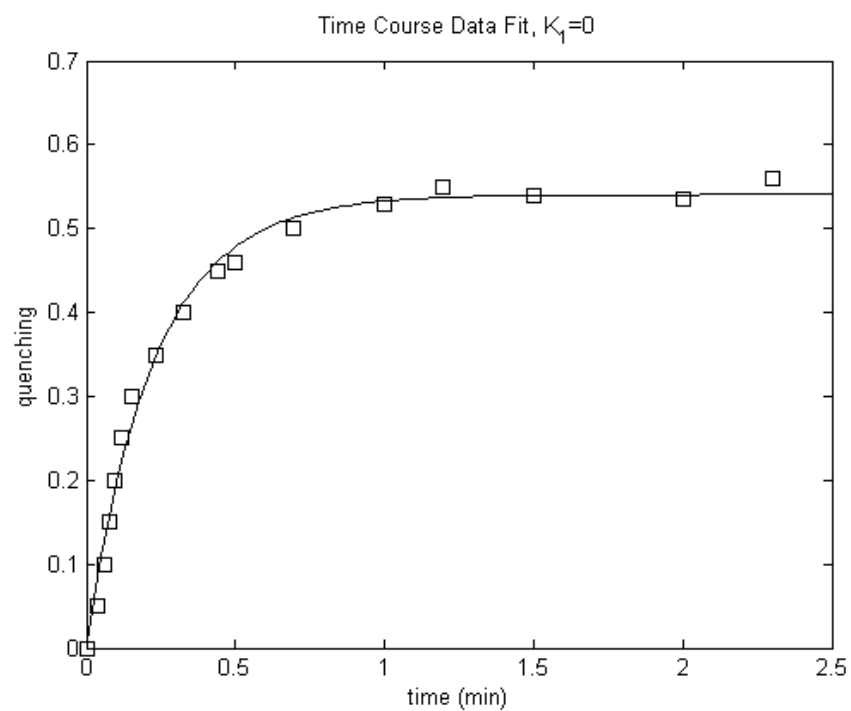


Figure 4.3: Time-dependent fit.

Chapter 5

Model Comparison

To analyze the model fits to equilibrium quenching data, we compare the sum of squared residual errors (SSR) for the various models. We also determine whether the additional terms in the Comprehensive model and Full model are significant to the data when compared to their nested models. In our first comparison, we consider the fit to data sets from quenching experiments measured under three conditions: AMP-PNP only, AMP-PNP with maltose, and no nucleotides with maltose ($n=36$), as shown in Figure 4.1. The Standard, Alternate, and Comprehensive model fits are compared for this first data set. In our second comparison, we consider the Comprehensive model and Full model fits to data sets measured under all four experimental conditions, as shown in Figure 4.2. This includes quenching data measured in the absence of nucleotides and without maltose present, which is omitted from the first comparison as only the Full model has quenching under conditions without nucleotides and without maltose.

5.1 Standard vs. Alternate

Both the Alternate model and Standard model have two equilibrium constants fit to quenching data, therefore we simply compare the SSR for the model fits of these parameters. The Alternate model is a better fit than the Standard model as it has a lower SSR of $9.8918 * 10^{-5}$ as seen in Table 5.1. This result is not surprising as the Standard model does not allow for the binding of unliganded MalE to the transporter, and is therefore insufficient to explain the quenching experiment performed in the presence of AMP-PNP, without maltose, in which strong quenching was observed. The Alternate model does not allow for the binding of MalE to maltose in the absence of nucleotides and therefore contradicts the quenching experimental

results performed in the absence of nucleotides.

Since the equilibrium quenching measured was less strong in the absence of nucleotides compared with AMP-PNP as shown in Figure 3.1, the error contributed to the Alternate model for omitting this reaction was small compared with the error contributed to the Standard model for omitting a Male-MalFGK₂ quenching reaction.

Model	Fit Parameters	SSR ₁	SSR ₂
Standard	K_3, K_4	0.0063	0.0065
Alternate	K_2, β	$9.8918 * 10^{-5}$	$3.2017 * 10^{-4}$
Comprehensive	K_2, β, K_3	$4.0025 * 10^{-5}$	$2.67 * 10^{-4}$
Full	K_2, β, K_3, δ		$4.7432 * 10^{-5}$

Table 5.1: Parameters fit to equilibrium nanodisc quenching data. SSR₁ gives the sum of the squared residual error (SSR) for the model fit to 3 experiments in conditions of AMP-PNP (with and without maltose) and without nucleotides (with maltose), and SSR₂ gives the SSR for model fits to all 4 experiments, including conditions without nucleotides (no maltose). The Full model has too many parameters to fit to only 3 experiments (therefore it has no SSR₁).

5.2 Alternate vs. Comprehensive

Our analysis of the Standard and Alternate model fits above to the equilibrium data show that the Comprehensive model, which includes all reactions from both models, will better explain the data measured in all three conditions described above. Comparing fits for AMP-PNP quenching experiments only, the Comprehensive model and Alternate model fit the data with the same SSR, indicating that the additional parameter in the Comprehensive model is not significant to the data when excluding data without nucleotides.

However, when we include the additional data set from the no nucleotides experiment in the presence of maltose, the Comprehensive model is clearly a better fit as seen in Figure 4.1. We use an F-test to compare the SSR for the fits as seen in Appendix E and find there is a statistically significant advantage of the Comprehensive model over the Alternate model

in predicting the experimental quenching data for the three data sets. The parameter K_3 , the equilibrium constant for binding liganded MalE to the closed transporter, is the additional equilibrium parameter in the Comprehensive model compared with the nested Alternate model. Equilibrium constant K_3 is found to be significant to the data ($p < 0.0001$). See Appendix E for analysis. We conclude that the Comprehensive model is a better fit to the data than the Alternate model, and that $K_3 \neq 0$ when comparing fits to experimental data measured in the presence of AMP-PNP, AMP-PNP (with maltose), and no nucleotides (with maltose).

5.3 Comprehensive vs. Full

We now compare the Full and Comprehensive models for the equilibrium parameter fits to all four quenching data sets as shown in Figure 4.2. See Table 5.1 for the SSR for each of these model fits. The Full model and Comprehensive model are fit to all 4 quenching experiments including the no nucleotides (no maltose) experiment. See Appendix E for analysis. We conclude that the Full model is a better fit to the data than the Comprehensive model when considering all four equilibrium experiments in the absence of nucleotides and in the presence of AMP-PNP. We conclude that the equilibrium parameter δ is nonzero in the reaction network of the maltose uptake system given by the Full model ($p < 0.0001$).

Chapter 6

Maltose Transport in Comprehensive Model

6.1 Analysis of Flux

Using nonlinear regression model fits we have shown that the Full and Comprehensive models provide superior fits to equilibrium quenching data compared with the Standard and Alternate models. Both the Full and Comprehensive models contain the following pathways for maltose transport: the standard, alternate, and open pathways.

Along the standard pathway, liganded MalE binds to the P-closed transporter to initiate maltose transport. The open pathway of transport is initiated by the binding of liganded MalE to the P-open transporter. The reverse reaction has been described as an autoregulatory step through which transport is inhibited at high maltose concentration. The alternate pathway of transport is for unliganded MalE to selectively bind the P-open transporter forming a high-affinity complex, and for maltose to subsequently bind and be imported to the cytosol.

We use experimental nanodisc data measured in the presence of ATP and maltose to analyze the flux through of each of these three pathways [1]. The Comprehensive model is used for this analysis as the available data are insufficient to estimate all of the additional kinetic parameters in the Full model shown in Table 2.4.

The ordinary differential equation system for the Comprehensive model is analyzed using equilibrium constants K_3 , K_2 , β and hydrolysis rates h_1 , h_2 , and h_3 , for the Comprehensive model as fit by nonlinear regression (see Chapter 4). The fit value for the binding rate of MalE to

P-open transporter k_2^+ from the time-dependent data as well as the estimate of the magnitude of k_1^+ were used for fixed K_1 values. Kinetic rates k_3^+ (binding of P-closed transporter to liganded MalE), and k_4^+ (conformation change from P-closed to P-open with E_m bound) are unknown. The binding rate of MalE to maltose, k_o^+ , has been measured experimentally at approximately $10^{-3} \text{ nm}^{-1} \text{ min}^{-1}$ [1]. The proportion of the equilibrium constant β applied to each of the associated backward rates, β_o, β_2 , as seen in Table 2.4 are unknown.

We want to determine the dominant pathway of maltose transport in the Comprehensive model for various cases of our unknown forward rates. In order to solve the ODE system at steady state, we take an asymptotics approach.

Using our fit hydrolysis rates, we have $h_1 < h_3 < h_2$, and we assume that the unknown forward rate k_1^+ is large such that $h_1 \ll k_1^+$. We estimated the magnitude of k_1^+ by choosing the fixed value with lowest SSR in the time-dependent fit (see Section 4.2.2). This analysis gives k_1^+ that is very large compared to h_1 , for all fixed K_1 values. We divide the steady state ODE system through by k_1^+ and regroup parameters. We let $\epsilon = \frac{h_1}{k_1^+}$ be a small parameter. We then let $\gamma = \frac{k_o^+}{k_1^+}$, $\alpha = \frac{k_2^+}{k_1^+}$, $\delta = \frac{k_3^+}{k_1^+}$, $\xi = \frac{k_4^+}{k_1^+}$. We let each concentration A, B, C, D, F, E, E_m be written as an asymptotic solution, $A = A_o + \epsilon A_1$, $B = B_o + \epsilon B_1$, ..., $E_m = E_{mo} + \epsilon E_{m1}$, and substitute into the steady state ODE system. The resulting system and expressions for values of A, B, \dots, E_m , can be found in Appendix F. They depend on k_j^+ , $j = 0, 1, 2, 3, 4$, the kinetic binding rates, the solutions to the steady state system at equilibrium found in Appendix C, and on the equilibrium constants, K_i .

We now calculate the flux through each pathway of the full model. We first label the fluxes as follows:

$$A \xrightarrow{f_1} B \xrightarrow{f_2} C \xrightarrow{f_3} F \xrightarrow{g_{3a}}, f_3 = \text{alternate pathway flux}$$

$$A \xrightarrow{f_5} D \xrightarrow{f_5} F \xrightarrow{g_{3s}}, f_5 = \text{standard pathway flux}$$

$$B \xrightarrow{f_4} F \xrightarrow{g_{3o}}, f_4 = \text{open pathway flux}$$

$$B \xrightarrow{g_1} A$$

$$C \xrightarrow{g_2} A$$

At steady state we have the following system of equations, where $g_1 = h_1 B$, $g_2 = h_2 C$, $g_3 = h_3 F$, and $g_3 = g_{3s} + g_{3a} + g_{3o}$:

$$f_1 = f_4 + f_2 + g_1$$

$$f_2 = f_3 + g_2$$

$$f_3 + f_4 + f_5 = g_3.$$

We can write the fluxes f_2 , f_4 as the following differences:

$$f_2 = k_2^+ BE - k_2^- C$$

$$f_4 = \beta_2 k_2^+ BE_m - \beta_2 \beta k_2^- F$$

Substitution of our asymptotic solutions gives the following approximation of the fluxes at steady state:

$$f_2 = k_2^+ (B_o + \epsilon B_1)(E_o + \epsilon E_1) - k_2^- (C_o + \epsilon C_1)$$

$$f_3 = f_2 - g_2$$

$$f_4 = \beta_2 k_2^+ (B_o + \epsilon B_1)(E_{m_o} + \epsilon E_{m_1}) - \beta_2 \beta k_2^- (F_o + \epsilon F_1).$$

$$f_5 = g_3 - f_4 - (f_2 - g_2)$$

The concentrations $B_1, E_1, C_1, F_1, E_{m_1}$ are found for fixed $K_1 = \{0.01, 0.1, 1, 100\}$ and for the fixed k_1^+ value found to have the lowest SSR as shown in Table 4.6. All related equilibrium fit values and k_2^+ fit value are used for each fixed K_1 .

The remaining unknowns for the flux calculation include k_3^+ , k_4^+ , β_o , and β_2 . The total maltose transport was calculated for fixed k_o^+ , β_o and β_2 , where:

$$C + M \xrightarrow{\beta_o k_o^+} F, \text{ and the reverse } F \xrightarrow{\beta_o \beta k_o^-} C + M$$

$$B + E_m \xrightarrow{\beta_2 k_2^+} F, \text{ and the reverse } F \xrightarrow{\beta_2 \beta k_2^-} B + E_m.$$

The parameters β_o , β_2 control the proportion of the equilibrium fit value β that is applied to the forward and backward rates for the above reactions. Thus we expect these two parameters to influence maltose flux through the alternate pathway (β_o) and the open pathway (β_2). For example, fixing $\beta_o = \beta_2 = 1$ assumes that only the backward kinetic rates shown above are affected by the fit equilibrium parameter β . We consider all the fixed cases such that $\beta_o = 0.01, 1, 100$ and $\beta_2 = 0.01, 1, 100$, to analyze the effect on the maltose flux along each pathway.

The direction and magnitude of the fluxes through each pathway were found to be relatively insensitive to the parameters k_3^+ and k_4^+ , and to the fixed values of β_o and β_2 . An experimental

value for k_o^+ , the forward binding rate of MalE to maltose, was used to compute the scaled flux through each pathway. The flux was not sensitive to values of k_o^+ greater than or equal to $10^{-4} \text{ nm}^{-1} \text{ min}^{-1}$, and the experimental value of $k_o^+ = 10^{-3} \text{ nm}^{-1} \text{ min}^{-1}$ falls within this range [1].

The standard pathway was negative for all fixed K_1 values less than or equal to 1, as seen in Figure 6.1. The open pathway was the dominant pathway of maltose transport for fixed $K_1 \leq 1$, and the alternate pathway makes a relatively small contribution to overall transport. The standard pathway was positive and the dominant pathway of maltose transport for the fixed case of $K_1 = 100$, as seen in Figure 6.2. For large K_1 the open pathway is still positive, and the alternate pathway has a small negative magnitude.

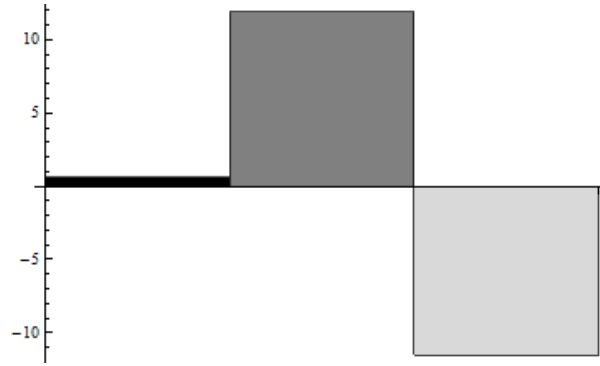


Figure 6.1: The scaled flux in the Comprehensive model, for fixed $K_1 = 0.1$ and $k_o^+ = 10^{-3} \text{ nm}^{-1} \text{ min}^{-1}$. For all fixed $K_1 \leq 1$, the open pathway (dark gray) was the dominant pathway, the standard pathway (light gray) was negative, and the alternate pathway (black) makes a small contribution to overall maltose transport.

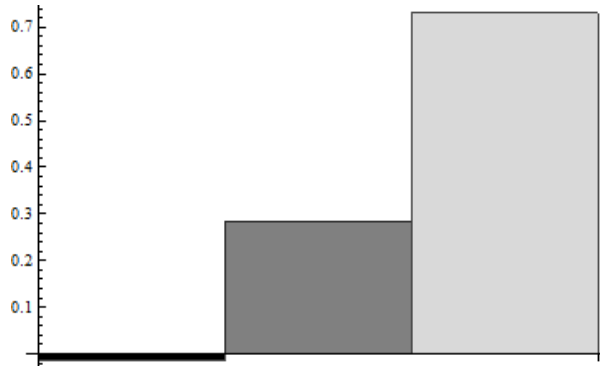


Figure 6.2: The scaled flux in the Comprehensive model, for fixed $K_1 = 100$ and $k_o^+ = 10^{-3} \text{ nm}^{-1} \text{ min}^{-1}$. For large K_1 only, the standard model (light gray) was the dominant pathway of maltose transport. The alternate pathway (black) is negative for large K_1 , and the open pathway (dark gray) is positive.

6.2 Further ATPase Results

Experiments have shown that MalE can inhibit transport in excess when maltose is held at sub-stoichiometric levels [7]. We replicate this result in the Comprehensive model as shown in Figure 6.3. Experiments have also shown that MalE increases the basal ATPase activity in NdFGK₂ (MalFGK₂ in nanodiscs) by 3-fold. These experiments also found that the in the presence of maltose, an inhibition of ATPase activity was observed in nanodiscs which was not observed in liposomes [1]. We replicate these results in the Comprehensive model as shown in Figure 6.3.

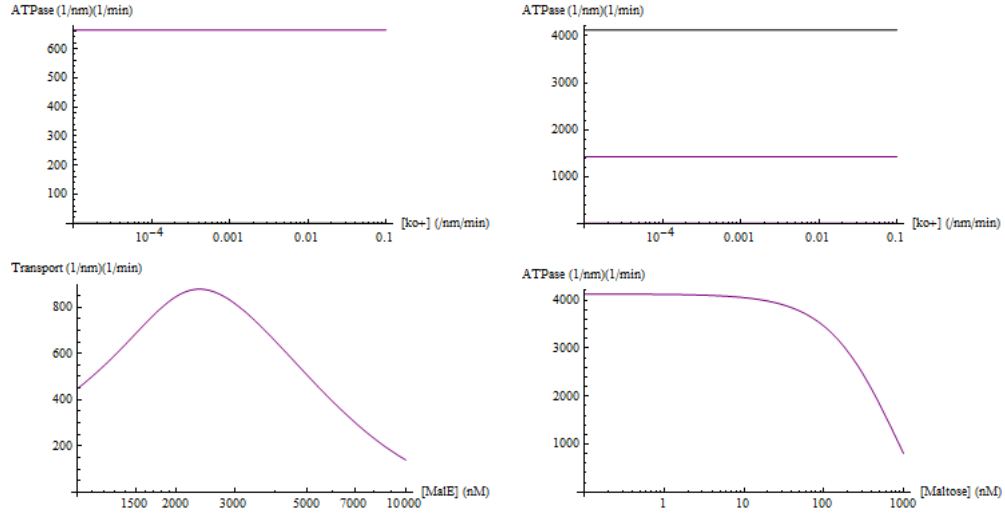


Figure 6.3: Comprehensive model results. (Top Left) Basal steady-state ATPase rate in the absence of MalE and in the absence of maltose. (Top Right) Total steady-state ATPase rate in the presence of 2 μ M MalE, without maltose (black) and ATPase rate of unbound transporter state $B \rightarrow A$ only in the presence of 2 μ M MalE (purple). (Bottom Left) Maltose transport inhibited for large concentrations of MalE, for fixed maltose concentration 2 μ M. (Bottom Right) ATPase activity is inhibited in the presence of maltose, for fixed MalE concentration 2 μ M.

Chapter 7

Discussion

Experimental data in nanodiscs have shown that the standard model of maltose transport, in which liganded MalE binds to the closed transporter to trigger a conformation change and deliver maltose, is insufficient to explain all binding interactions observed between MalE and MalFGK₂ in the absence of hydrolysis. Nonlinear regression fit analysis of four mathematical models has shown that models which include binding of unliganded MalE to the transporter produce significantly better fits to equilibrium data obtained from nanodisc experiments.

Additionally, it was shown that omission of the standard pathway of maltose transport in the Alternate model did not result in a better fit to equilibrium data when compared with the Comprehensive model. This indicates that the Alternate model is insufficient to explain experimental binding data in the absence of nucleotides. The Full model was shown to be a significantly better fit to equilibrium nanodisc data than the three models nested within it, as it provides binding reactions for MalE and maltose under all experimental conditions considered.

The nonlinear regression analysis confirms that a complex network of binding interactions can occur between the components of the maltose uptake system in E.coli when hydrolysis is blocked. The three possible pathways of maltose transport available within this network were analyzed using the Comprehensive model at steady state in the presence of ATP.

The direction and quantity of maltose flux through each available pathway was computed. Results were relatively insensitive to values of the unknown parameters k_3^+ and k_4^+ , and to fixed values of β_o and β_2 . The standard pathway was negative for fixed values of the equilibrium constant between P-open and P-closed conformations of the transporter, K_1 , less than or equal to 1. For large K_1 , the standard pathway was positive and the major pathway of maltose

transport.

The fit analysis to nanodisc time course data gave the best fit for fixed value $K_1 = 0.1$. For $K_1 = 0.1$, and for all fixed $K_1 \leq 1$, the open pathway was the major pathway of maltose transport. A relatively small flux of maltose was calculated along the alternate pathway. The negative flux along the standard pathway calculated in this range of small K_1 could represent a means of regulating maltose uptake at high concentrations, as proposed [1]. In reverse, the standard pathway involves binding of MalE to the maltose in the transporter pocket and subsequent closing of the transporter. Liganded MalE subsequently dissociates from the P-closed transporter, removing and regulating maltose import.

The open pathway of maltose transport would rely on an affinity of MalE for the P-open transporter, as observed in nanodisc quenching experiments performed under hydrolysis blocking conditions [1]. Perhaps this high affinity encourages the MalE-MalFGK₂ intermediate complex. The dominance of the open pathway indicates that the binding of ATP to the nucleotide-binding domain may close the transporter prior to the association of liganded MalE. We conclude that liganded MalE may selectively bind the P-open conformation of MalFGK₂ in the presence of nucleotides to initiate maltose transport, and that the standard pathway may in fact occur in reverse as a mode of regulating maltose import at high concentrations. We also conclude that some small amount of maltose import may occur along the alternate pathway.

For this analysis, an enhanced Michaelis-Menten formalism was used to fit ODE model parameters to experimental equilibrium data. Furthermore, the flux through the transport system was calculated using asymptotic analysis, fit parameter values, and experimentally measured values. Moreover, two apparently distinct models were compared and integrated, and the fluxes through potential transport pathways were calculated and compared. This type of analysis could be generalized to other biochemical transport systems to provide insight into detailed binding networks using biochemical data, and to distinguish between possible transport pathways in cases where available data may conflict with accepted models of biochemical transport.

Bibliography

- [1] Bao H, Duong F (2012) Discovery of an Auto-Regulation Mechanism for the Maltose ABC Transporter *MalFGK₂*. PLoS ONE 7(4): e34836. doi:10.1371/ journal.pone.0034836
- [2] Locher K (2004) Structure and Mechanism of ABC transporters. Current Opinion in Structural Biology 14(4): 0959-440X. doi: 10.1016/j.sbi.2004.06.005
- [3] Shilton B (2008) The dynamics of MBP MalFGK2 interaction: A prototype for binding protein dependent ABC-transporter systems. Biochimica et Biophysica Acta (BBA)-Biomembranes 1778(9): 0005-2736. doi:10.1016/j.bbamem.2007.09.005
- [4] Oldham M, Khare D, Florante Q, Davidson A, Chen J (2007) Crystal Structure of a catalytic intermediate of the maltose transporter. Nature 450: doi:10.1038/nature06264
- [5] Oldham M, Chen J (2011) Crystal structure of the maltose transporter in a pretranslocation intermediate state. Science 332: 1202-1205.
- [6] Orelle C, Ayvaz T, Everly RM, Klug CS, Davidson AL (2008) Both maltose-binding protein and ATP are required for nucleotide-binding domain closure in the intact maltose ABC transporter. Proc Natl Acad Sci U S A 105: 12837-12842.
- [7] Merino G, Shuman HA (1997) Unliganded maltose-binding protein triggers lactose transport in an Escherichia coli mutant with an alteration in the matose transport system. J Bacteriol 179: 7687-7694
- [8] Merino G, Boos W, Shuman HA, Bohl E (1995) The inhibition of maltose transport by the unliganded form of the maltose-binding protein of Escherichia coli: experimental findings and mathematicak treatment. J Theor Biol 177: 171-179.
- [9] Austermuhle MI, Hall JA, Klug CS, Davidson AL (2004) Maltose-binding protein is open in the catalytic transition state for ATP hydrolysis during maltose transport. J Biol Chem 279: 28243-28250.

- [10] Bohl E, Shuman H, Boos W (1994) Mathematical Treatment of the Kinetics of Binding Protein Dependent Transport Systems Reveals that Both the Substrate Loaded and Unloaded Binding Proteins Interact with Membrane Components. *J Theor Biol* 172: 83-94.
- [11] Bohl E, Boos W (1997) Quantitative Analysis of Binding Protein-mediated ABC Transport Systems. *J Theor Biol* 186: 65-74.
- [12] Gould A, Telmer P, Shilton B (2010) Simulation of the Maltose Transporter ATPase by Unliganded Maltose Binding Protein. *Biochemistry* 49: 653-820.
- [13] Bayburt T, Sligar S (2010) Membrane Protein Assembly into Nanodiscs. *FEBS Letters* 548:1721-1727
- [14] Marme N, Kneneyer JP, Sauer M, Wolfram J(2003) Inter- and intramolecular fluorescence quenching of organic dyes by tryptophan. *Bioconjug Chem* 14: 1133-1139.

Appendix A

Standard Model

The concentrations of each state in the Standard model at equilibrium were found using the following equalities and conservation equations:

$$D = \frac{AE_m}{K_3}, F = \frac{D}{K_4}, E = \frac{E_m K_o}{M}$$

$$A + D + F = T_o$$

$$E + D + F + E_m = E_o$$

Now,

$$A = T_o - D - \frac{D}{K_4} = T_o - D(1 + \frac{1}{K_4})$$

$$E + E_m + D + F = E_o$$

$$\frac{E_m K_o}{M} + E_m + D + \frac{D}{K_4} = E_o$$

$$E_m(\frac{K_o}{M} + 1) + D(1 + \frac{1}{K_4}) = E_o$$

let $\gamma = \frac{K_o}{M} + 1$, $\omega = 1 + \frac{1}{K_4}$, then

$$\gamma E_m + \omega D = E_o$$

$$E_m = \frac{E_o - \omega D}{\gamma}$$

$$K_3 D = A E_m$$

$$K_3 D = (T_o - \omega D)(\frac{E_o - \omega D}{\gamma})$$

$$K_3 D \gamma = (T_o - \omega D)(E_o - \omega D)$$

$$K_3 D \gamma = T_o E_o - \omega D E_o - \omega D T_o + \omega^2 D^2$$

$$0 = T_o E_o - \omega D E_o - \omega D T_o + \omega^2 D^2 - K_3 D \gamma$$

$$0 = \omega^2 D^2 - D(\omega E_o + \omega T_o + K_3 \gamma) + T_o E_o$$

$$0 = D^2 - D\left(\frac{E_o}{\omega} + \frac{T_o}{\omega} + \frac{K_3 \gamma}{\omega^2}\right) + \frac{T_o E_o}{\omega^2}$$

$$D = 0.5(b \pm \sqrt{b^2 - 4c})$$

$$\text{where } b = \frac{E_o}{\omega} + \frac{T_o}{\omega} + \frac{K_3 \gamma}{\omega^2}, c = \frac{T_o E_o}{\omega^2}$$

Nondimensional Standard Model

$$\text{Let } D = dE_o, A = aE_o, F = fE_o, E = eE_o, E_m = jE_o$$

where d, a, f, e, and j are dimensionless variables. Let $\rho = \frac{T_o}{E_o}$.

Then:

$$d = 0.5\left(\frac{b}{E_o} \pm \sqrt{\left(\frac{b}{E_o}\right)^2 - 4\frac{c}{E_o^2}}\right)$$

where:

$$\frac{b}{E_o} = \frac{1}{\omega} + \frac{\rho}{\omega} + \frac{K_3^* \gamma}{\omega^2}$$

$$\frac{c}{E_o^2} = \frac{\rho}{\omega^2}.$$

$$a = \rho - \omega d$$

$$f = \frac{d}{K_4}$$

$$j = \frac{1 - \omega d}{\gamma}$$

$$e = \frac{j K_o}{M}$$

Appendix B

Alternate Model

The concentrations of each state in the Alternate model at equilibrium were found using the following equalities and conservation equations:

$$A = K_1 B$$

$$BE = K_2 C$$

$$BE_m = \beta K_2 F$$

$$\beta K_o F = CM$$

$$EM = K_o E_m$$

$$A + B + C + F = T_t$$

$$E + E_m + C + F = E_t$$

$$E + \frac{EM}{K_o} + C + \frac{M}{K_o \beta} C = E_o$$

$$\xi E + \nu C = E_o, \text{ where } \xi = 1 + \frac{M}{K_o}, \nu = 1 + \sigma$$

$$E = \frac{E_o - \nu C}{\xi}$$

$$E_m = \frac{EM}{K_o}$$

$$B = K_2 C \frac{\xi}{E_o - \nu C}$$

$$A = K_1 B$$

$$F = \sigma C$$

Now

$$A + B + C + F = T_o$$

$$K_1 B + B + C + \sigma C = T_o$$

$$B(K_1 + 1) + C(1 + \sigma) = T_o$$

$$\text{Let } \psi = K_2(K_1 + 1),$$

$$\frac{\psi C \xi}{E_o - \nu C} + \nu C = T_o$$

$$\psi C \xi + \nu C(E_o - \nu C) = T_o(E_o - \nu C)$$

$$\psi C \xi + \nu E_o C - \nu^2 C^2 = T_o E_o - \nu T_o C$$

$$\psi C \xi + \nu E_o C - \nu^2 C^2 - T_o E_o + \nu T_o C = 0$$

$$-\nu^2 C^2 + C(\psi \xi + \nu E_o + \nu T_o) - T_o E_o = 0$$

$$C^2 - C(\frac{\psi \xi}{\nu^2} + \frac{E_o}{\nu} + \frac{T_o}{\nu}) + \frac{T_o E_o}{\nu^2} = 0$$

$$C = 0.5[(\frac{\psi \xi}{\nu^2} + \frac{E_o}{\nu} + \frac{T_o}{\nu}) \pm \sqrt{(\frac{\psi \xi}{\nu^2} + \frac{E_o}{\nu} + \frac{T_o}{\nu})^2 - \frac{4T_o E_o}{\nu^2}}]$$

Nondimensional Alternate Model

Let $C = cE_o, B = bE_o, A = aE_o, F = fE_o, E_m = jE_o, E = eE_o$ where c,b,a,f,j, and e are dimensionless variables. Let $\rho = \frac{T_o}{E_o}, \eta = \frac{\psi}{E_o}$.

Then:

$$c = 0.5[(\frac{\eta \xi}{\nu^2} + \frac{1}{\nu} + \frac{\rho}{\nu}) \pm \sqrt{(\frac{\eta \xi}{\nu^2} + \frac{1}{\nu} + \frac{\rho}{\nu})^2 - \frac{4\rho}{\nu^2}}]$$

$$f = \sigma c$$

Appendix C

Comprehensive Model

The concentrations of each state in the Comprehensive model at equilibrium were found using the following equalities and conservation equations:

$$A = K_1 B$$

$$BE = K_2 C$$

$$BE_m = \beta K_2 F$$

$$\beta K_o F = CM$$

$$D = K_4 F$$

$$E + E_m + C + D + F = E_o$$

$$A + B + C + D + F = T_o$$

$$F = \sigma C, \text{ where } \sigma = \frac{M}{K_o \beta}$$

$$E_m = \frac{EM}{K_o}$$

$$E + \frac{EM}{K_o} + C + K_4 \sigma C + \sigma C = E_o$$

$$E(1 + \frac{M}{K_o}) + C(1 + K_4 \sigma + \sigma) = E_o$$

$$\xi E + \alpha C = E_o, \text{ where } \xi = 1 + \frac{M}{K_o}, \alpha = 1 + \sigma(K_4 + 1)$$

$$E = \frac{E_o - \alpha C}{\xi}$$

$$B = \frac{K_2 C \xi}{E_o - \alpha C}$$

Now

$$A + B + C + D + F = T_o$$

$$K_1 B + B + C + K_4 \sigma C + \sigma C = T_o$$

$$B(K_1 + 1) + C(1 + K_4 \sigma + \sigma) = T_o$$

$$\text{Let } \psi = K_2(K_1 + 1)$$

$$\frac{\psi C \xi}{E_o - \alpha C} + \alpha C = T_o$$

$$\psi C \xi + \alpha C(E_o - \alpha C) = T_o(E_o - \alpha C)$$

$$\psi C \xi + \alpha E_o C - \alpha^2 C^2 = T_o E_o - \alpha T_o C$$

$$\psi C \xi + \alpha E_o C - \alpha^2 C^2 - T_o E_o + \alpha T_o C = 0$$

$$-\alpha^2 C^2 + C(\psi \xi + \alpha E_o + \alpha T_o) - T_o E_o = 0$$

$$C^2 - C\left(\frac{\psi \xi}{\alpha^2} + \frac{E_o}{\alpha} + \frac{T_o}{\alpha}\right) + \frac{T_o E_o}{\alpha^2} = 0$$

$$C = 0.5\left[\left(\frac{\psi \xi}{\alpha^2} + \frac{E_o}{\alpha} + \frac{T_o}{\alpha}\right) \pm \sqrt{\left(\frac{\psi \xi}{\alpha^2} + \frac{E_o}{\alpha} + \frac{T_o}{\alpha}\right)^2 - \frac{4T_o E_o}{\alpha^2}}\right]$$

$$\text{Let } \kappa = \sigma(1 + K_4)$$

Nondimensional Full Model

Let $C = cE_o, B = bE_o, A = aE_o, F = fE_o, D = dE_o E_m = jE_o, E = eE_o$ where c,b,d,a,f,j, and e are dimensionless variables. Let $\rho = \frac{T_o}{E_o}, \eta = \frac{\psi}{E_o}$.

Then:

$$c = 0.5\left[\left(\frac{\eta \xi}{\alpha^2} + \frac{1}{\alpha} + \frac{\rho}{\alpha}\right) \pm \sqrt{\left(\frac{\eta \xi}{\alpha^2} + \frac{1}{\alpha} + \frac{\rho}{\alpha}\right)^2 - \frac{4\rho}{\alpha^2}}\right]$$

$$f = \sigma c$$

$$d = K_4 \sigma c$$

No nucleotides derivation:

$$A = \frac{K_3 D}{E_m}$$

$$E = \frac{E_m K_o}{M}$$

$$A + B + C + D + F = T_o$$

$$\frac{K_3 D}{E_m} + 0 + 0 + D + 0 = T_o$$

$$\frac{K_3 d E_o}{j E_o} + d E_o = T_o$$

$$\frac{K_3 d}{j} + d E_o = T_o$$

$$\frac{K_3^* d}{j} + d = \rho, \text{ where } K_3^* = \frac{K_3}{E_o}$$

$$E + E_m + C + D + F = E_o$$

$$\frac{E_m K_o}{M} + E_m + 0 + D + 0 = E_o$$

$$E_m \left(\frac{K_o}{M} + 1 \right) + D = E_o$$

$$j E_o \left(\frac{K_o}{M} + 1 \right) + d E_o = E_o$$

$$j \left(\frac{K_o}{M} + 1 \right) + d = 1, \text{ let } \frac{K_o}{M} + 1 = \omega$$

$$j \omega + d = 1$$

$$j = \frac{1-d}{\omega}$$

$$\frac{K_3^* \omega d}{1-d} + d = \rho$$

$$K_3^* \omega d + d(1-d) = \rho(1-d)$$

$$K_3^* \omega d + d - d^2 = \rho - \rho d$$

$$K_3^* \omega d + d - d^2 - \rho + \rho d = 0$$

$$-d^2 + d(K_3^* \omega + 1 + \rho) - \rho = 0$$

$$d^2 - d(K_3^* \omega + 1 + \rho) + \rho = 0$$

$$d = 0.5((K_3^* \omega + 1 + \rho) - \sqrt{(K_3^* \omega + 1 + \rho)^2 - 4\rho})$$

Other Model with assumption that AMP-PNP closes interface

$K_4, K_1 \rightarrow 0$, therefore $A \rightarrow 0$ and $D \rightarrow 0$

1)AMP-PNP: $B + C = T_o$

$$E + C = E_o, E = E_o - C$$

$$\frac{K_2 C}{E} + C = T_o$$

$$K_2 C + EC = ET_o$$

$$K_2 C + (E_o - C)C = (E_o - C)T_o$$

$$K_2 C + E_o C - C^2 = E_o T_o - T_o C$$

$$-C^2 + C(K_2 + E_o + T_o) - E_o T_o = 0$$

$$C^2 - C(K_2 + E_o + T_o) + E_o T_o = 0$$

$$(cE_o)^2 - cE_o(K_2 + E_o + T_o) + E_o T_o = 0$$

$$c^2 - c(K_2^* + 1 + \rho) + \rho = 0$$

$$c = (K_2^* + 1 + \rho) - \sqrt{b^2 - 4\rho}$$

2)AMP+Malt: $B + C + F = T_o$

$$E + E_m + C + F = E_o$$

$$E + \frac{EM}{K_o} + C + \sigma C = E_o$$

$$E = \frac{E_o - C(1+\sigma)}{\gamma}$$

$$\frac{K_2 C}{E} + C + \sigma C = T_o$$

$$K_2 C + C\left(\frac{E_o - C(1+\sigma)}{\gamma}\right)(1 + \sigma) = T_o\left(\frac{E_o - C(1+\sigma)}{\gamma}\right)$$

$$K_2 C + \frac{E_o C(1+\sigma)}{\gamma} - \frac{C^2(1+\sigma)^2}{\gamma} = \frac{T_o E_o}{\gamma} - \frac{CT_o(1+\sigma)}{\gamma}$$

$$K_2 C + \frac{E_o C(1+\sigma)}{\gamma} - \frac{C^2(1+\sigma)^2}{\gamma} + \frac{CT_o(1+\sigma)}{\gamma} - \frac{T_o E_o}{\gamma} = 0$$

$$-C^2 \frac{(1+\sigma)^2}{\gamma} + C\left(K_2 + \frac{E_o(1+\sigma)}{\gamma} + \frac{T_o(1+\sigma)}{\gamma}\right) - \frac{T_o E_o}{\gamma} = 0$$

$$C^2(1 + \sigma)^2 - C(K_2 \gamma + E_o(1 + \sigma) + T_o(1 + \sigma)) + T_o E_o = 0$$

$$C^2 - C(\frac{K_2\gamma}{(1+\sigma)^2} + \frac{E_o}{(1+\sigma)} + \frac{T_o}{(1+\sigma)}) + \frac{T_o E_o}{(1+\sigma)^2} = 0$$

Nondimensionalize:

$$(cE_o)^2 - cE_o(\frac{K_2\gamma}{(1+\sigma)^2} + \frac{E_o}{(1+\sigma)} + \frac{T_o}{(1+\sigma)}) + \frac{T_o E_o}{(1+\sigma)^2} = 0$$

$$c^2 - c(\frac{K_2^*\gamma}{(1+\sigma)^2} + \frac{1}{(1+\sigma)} + \frac{\rho}{(1+\sigma)}) + \frac{\rho}{(1+\sigma)^2} = 0$$

$$c = 0.5[(\frac{K_2^*\gamma}{(1+\sigma)^2} + \frac{1}{(1+\sigma)} + \frac{\rho}{(1+\sigma)}) - \sqrt{b^2 - \frac{4\rho}{(1+\sigma)^2}}]$$

$$\text{quenching: } \frac{c+f}{\phi} = \frac{c(1+\sigma)}{\phi}$$

Appendix D

Full Model

The concentrations of each state in the Full model at equilibrium were found using the following equalities and conservation equations:

$$A = K_1 B$$

$$BE = K_2 C$$

$$BE_m = \beta K_2 F$$

$$\beta K_o F = CM$$

$$D = K_4 F$$

$$AE = \frac{K_3}{\delta} G$$

$$AE_m = K_3 D$$

$$E + E_m + C + D + F + G = E_o$$

$$A + B + C + D + F + G = T_o$$

$$F = \sigma C, \text{ where } \sigma = \frac{M}{K_o \beta}$$

$$E_m = \frac{EM}{K_o}$$

For the Full model we must use the stronger assumption that AMP-PNP stabilizes the P-open conformation in order to fit the data.

In the absense of nucleotides, we assume we have only P-closed states:

$$A + D + G = T_t$$

$$E + E_m + D + G = E_t$$

$$A = \frac{K_3}{\delta E} G$$

$$D = \frac{M}{\delta K_o} G$$

$$\frac{K_3}{\delta E} G + \frac{M}{\delta K_o} G + G = T_t$$

$$E + \frac{EM}{K_o} + \frac{M}{\delta K_o} G + G = E_t$$

$$E(1 + \frac{M}{K_o}) + G(1 + \frac{M}{\delta K_o}) = E_t,$$

$$E\gamma + G\xi = E_t, \text{ where } \xi = 1 + \frac{M}{\delta K_o}, \gamma = 1 + \frac{M}{K_o}$$

$$E = \frac{E_t - \xi G}{\gamma}$$

$$\frac{K_3}{\delta E} G + \frac{M}{\delta K_o} G + G = T_t$$

$$\frac{K_3}{\delta} \frac{\gamma}{E_t - \xi G} G + G\xi = T_t$$

$$K_3\gamma G + G\xi\delta(E_t - \xi G) = T_t\delta(E_t - \xi G)$$

$$K_3\gamma G + G\xi\delta E_t - \xi^2 G^2\delta - T_t\delta E_t + T_t\delta\xi G = 0$$

$$\xi^2\delta G^2 - G(K_3\gamma + \xi\delta E_t + T_t\delta\xi) + T_tE_t\delta = 0$$

$$G^2 - G \frac{(K_3\gamma + \xi\delta E_t + T_t\delta\xi)}{\xi^2\delta} + \frac{T_tE_t\delta}{\xi^2\delta} = 0$$

$$G = 0.5[(\frac{K_3\gamma}{\xi^2\delta} + \frac{E_t}{\xi} + \frac{T_t}{\xi}) \pm \sqrt{(\frac{K_3\gamma}{\xi^2\delta} + \frac{E_t}{\xi} + \frac{T_t}{\xi})^2 - \frac{4T_tE_t}{\xi^2}}]$$

Nondimensionalize: let g, d be nondimensional variables such that $G = gE_t$, $D = dE_t$ and let $\rho = \frac{T_t}{E_t}$, $K_3^* = \frac{K_3}{E_t}$. Then,

$$g = 0.5[(\frac{K_3^*\gamma}{\xi^2\delta} + \frac{1}{\xi} + \frac{\rho}{\xi}) \pm \sqrt{(\frac{K_3^*\gamma}{\xi^2\delta} + \frac{1}{\xi} + \frac{\rho}{\xi})^2 - \frac{4\rho}{\xi^2}}]$$

$$d = \frac{M}{\delta K_o} g$$

$$\text{quenching: } \frac{g+d}{\phi} = \frac{g(1+\frac{M}{\delta K_o})}{\phi}.$$

In the presence of AMP-PNP, we assume that we have only P-open states at equilibrium. Therefore in the presence of AMP-PNP the Full model is identical to the Comprehensive model.

Appendix E

F-test

$SSR_{Alternate}$	$9.8918 * 10^{-5}$	$SSR_{Comprehensive}$	$2.6127 * 10^{-4}$
$SSR_{Comprehensive}$	$4.0025 * 10^{-5}$	SSR_{Full}	$4.7432 * 10^{-5}$
n	36	n	48
F	47.085	F	193.8572
v_1	1	v_1	1
v_2	32	v_2	43
$F_{0.00001, v_1, v_2}$	27.41602865	$F_{0.00001, v_1, v_2}$	25.03720916
p	0.00000009	p	$< 10^{-8}$

Table E.1: F-test values for comparing the Alternate and Comprehensive models (left) and for comparing the Comprehensive and Full models (right).

Appendix F

Flux Calculation

The Comprehensive Model has the following ODE system, with $\beta = \frac{\beta_1}{\beta_o}$, $\beta = \frac{\beta_3}{\beta_2}$.

$$\frac{dA}{dt} = -k_1^+ A + k_1^- B - k_3^+ A E_m + k_3^- D + h_1 B + h_2 C + h_3 F$$

$$\frac{dB}{dt} = k_1^+ A - k_1^- B - k_2^+ B E + k_2^- C - \beta_2 k_2^+ B E_m + \beta_3 k_2^- F - h_1 B$$

$$\frac{dC}{dt} = -k_2^- C + k_2^+ B E - \beta_o k_o^+ C M + \beta_1 k_o^- F - h_2 C$$

$$\frac{dD}{dt} = k_3^+ E_m A - k_3^- D - k_4^+ D + k_4^- F$$

$$\frac{dF}{dt} = \beta_2 k_2^+ B E_m - \beta_3 k_2^- F + k_4^+ D - k_4^- F - h_3 F + \beta_o k_o^+ C M - \beta_1 k_o^- F$$

$$\frac{dE}{dt} = -k_o^+ E M + k_o^- E_m - k_2^+ B E + k_2^- C + h_2 C + h_3 F$$

$$\frac{dE_m}{dt} = -k_3^+ E_m A + k_3^- D - \beta_2 k_2^+ B E_m + \beta_3 k_2^- F + k_o^+ E M - k_o^- E_m$$

$$A + B + C + D + F = T_t$$

$$E + E_m + C + D + F = E_t$$

We now consider the steady state system with hydrolysis:

$$0 = -k_1^+ A + k_1^- B - k_3^+ A E_m + k_3^- D + h_1 B + h_2 C + h_3 F$$

$$0 = k_1^+ A - k_1^- B - k_2^+ B E + k_2^- C - \beta_2 k_2^+ B E_m + \beta_3 k_2^- F - h_1 B$$

$$0 = -k_2^- C + k_2^+ B E - \beta_o k_o^+ C M + \beta_1 k_o^- F - h_2 C$$

$$0 = k_3^+ E_m A - k_3^- D - k_4^+ D + k_4^- F$$

$$0 = \beta_2 k_2^+ B E_m - \beta_3 k_2^- F + k_4^+ D - k_4^- F - h_3 F + \beta_o k_o^+ C M - \beta_1 k_o^- F$$

$$0 = -k_o^+ E M + k_o^- E_m - k_2^+ B E + k_2^- C + h_2 C + h_3 F$$

$$0 = -k_3^+ E_m A + k_3^- D - \beta_2 k_2^+ B E_m + \beta_3 k_2^- F + k_o^+ E M - k_o^- E_m$$

$$A + B + C + D + F = T_t$$

$$E + E_m + C + D + F = E_t$$

Using our fit hydrolysis rates, we have $h_1 < h_3 < h_2$, and we assume that the unknown forward rate k_1^+ is large such that $h_1 \ll k_1^+$. Our previous analysis of k_1^+ in the time course quenching data supports this assumption that k_1^+ is large compared to h_1 , for all fixed K_1 values. We divide the steady state system through by k_1^+ and regroup parameters. We let $\epsilon = \frac{h_1}{k_1^+}$ be a small parameter. We then let $\gamma = \frac{k_o^+}{k_1^+}$, $\alpha = \frac{k_2^+}{k_1^+}$, $\delta = \frac{k_3^+}{k_1^+}$, $\xi = \frac{k_4^+}{k_1^+}$, and have the resulting steady state system (1):

$$0 = -A + K_1 B - \delta E_m A + K_3 \delta D + \epsilon B + \rho \epsilon C + w \epsilon F$$

$$0 = A - K_1 B - \alpha B E + \alpha K_2 C - \alpha \beta_2 B E_m + \alpha \beta \beta_2 K_2 F - \epsilon B$$

$$0 = -K_2 \alpha C + \alpha B E - \gamma \beta_o C M + \beta_o \beta K_o \gamma F - \rho \epsilon C$$

$$0 = \delta E_m A - K_3 \delta D - \xi D + K_4 \xi F$$

$$0 = \alpha \beta_2 B E_m - \beta_2 \beta K_2 \alpha F + \xi D - K_4 \xi F + \gamma \beta_o C M - \beta_o \beta \gamma K_o F - w \epsilon F$$

$$0 = -\gamma E M + K_o \gamma E_m - \alpha B E + K_2 \alpha C + \rho \epsilon C + w \epsilon F$$

$$0 = -\delta E_m A + K_3 \delta D - \alpha \beta_2 B E_m + \beta_2 \beta K_2 \alpha F + \gamma E M - \gamma K_o E_m$$

$$A + B + C + D + F = T_t$$

$$E + E_m + C + D + F = E_t$$

We let each concentration A, B, C, D, F, E, E_m be written as an asymptotic solution, $A = A_o + \epsilon A_1$, $B = B_o + \epsilon B_1$, ..., $E_m = E_{m_o} + \epsilon E_{m_1}$, and substitute into (1). We then consider the O(o) system:

$$0 = -A_o + K_1 B_o - \delta E_{m_o} A_o + K_3 \delta D_o$$

$$0 = A_o - K_1 B_o - \alpha B_o E_o + \alpha K_2 C_o - \alpha \beta_2 B_o E_{m_o} + \beta_2 \beta \alpha K_2 F_o$$

$$0 = -K_2 \alpha C_o + \alpha B_o E_o - \gamma \beta_o C_o M + \beta_o \beta K_o \gamma F_o$$

$$0 = \delta E_{m_o} A_o - K_3 \delta D_o - \xi D_o + K_4 \xi F_o$$

$$0 = \alpha \beta_2 B_o E_{m_o} - \beta_2 \beta K_2 \alpha F_o + \xi D_o - K_4 \xi F_o + \beta_o \gamma C_o M - \beta_o \beta \gamma K_o F_o$$

$$0 = -\gamma E_o M + K_o \gamma E_{m_o} - \alpha B_o E_o + K_2 \alpha C_o$$

$$0 = -\delta E_{m_o} A_o + K_3 \delta D_o - \alpha \beta_2 B_o E_{m_o} + \beta_2 \beta K_2 \alpha F_o + \gamma E_o M - \gamma K_o E_{m_o}$$

$$A_o + B_o + C_o + D_o + F_o = T_t$$

$$E_o + E_{m_o} + C_o + D_o + F_o = E_t$$

The O(o) system is the quasi-steady state system, in this case it is equivalent to the system at equilibrium without hydrolysis. We have assumed that the hydrolysis rates are slow. We use our previously derived solutions to the equilibrium system:

$$A_o, B_o, C_o, D_o, F_o, E_o, E_{m_o} = f(T_t, E_t, M, K_i, \beta),$$

Where K_i , $i = 0, 1, 2, 3, 4$, are the equilibrium ratios.

We now consider the O(1) system:

$$0 = -A_1 + K_1 B_1 - \delta(E_{m_o} A_1 + E_{m_1} A_o) + K_3 \delta D_1 + B_o + \rho C_o + w F_o$$

$$0 = A_1 - K_1 B_1 - \alpha(B_o E_1 + B_1 E_o) + \alpha K_2 C_1 - \alpha \beta_2(B_o E_{m_1} + B_1 E_{m_o}) + \beta_2 \beta \alpha K_2 F_1 - B_o$$

$$0 = -K_2 \alpha C_1 + \alpha(B_o E_1 + B_1 E_o) - \beta_o \gamma C_1 M + \beta_o \beta K_o \gamma F_1 - \rho C_o$$

$$0 = \delta(E_{m_o} A_1 + E_{m_1} A_o) - K_3 \delta D_1 - \xi D_1 + K_4 \xi F_1$$

$$0 = \alpha \beta_2(B_o E_{m_1} + B_1 E_{m_o}) - \beta_2 \beta K_2 \alpha F_1 + \xi D_1 - K_4 \xi F_1 + \beta_o \gamma C_1 M - \beta_o \beta \gamma K_o F_1 - w F_o$$

$$0 = -\gamma E_1 M + K_o \gamma E_{m_1} - \alpha(B_o E_1 + B_1 E_o) + K_2 \alpha C_1 + \rho C_o + w F_o$$

$$0 = -\delta(E_{m_o} A_1 + E_{m_1} A_o) + K_3 \delta D_1 - \alpha \beta_2(B_o E_{m_1} + B_1 E_{m_o}) + \beta_2 \beta K_2 \alpha F_1 + \gamma E_1 M - \gamma K_o E_{m_1}$$

$$A_1 + B_1 + C_1 + D_1 + F_1 = 0$$

$$E_1 + E_{m_1} + C_1 + D_1 + F_1 = 0$$

This system is linear, and can be reduced using the conservation equations. We let $A_1 = -(B_1 + C_1 + D_1 + F_1)$, $E_{m1} = -(E_1 + C_1 + D_1 + F_1)$, and reduce the $O(1)$ system to:

$$B_1 p_1 + C_1 p_2 + D_1 p_3 + F_1 p_4 - B_o = 0$$

$$B_1 p_5 + C_1 p_6 + E_1 p_7 + F_1 p_8 - \rho C_o = 0$$

$$B_1 p_9 + C_1 p_{10} + D_1 p_{11} + E_1 p_{12} + F_1 p_{13} = 0$$

$$B_1 p_{14} + C_1 p_{15} + D_1 p_{16} + E_1 p_{17} + F_1 p_{18} - w F_o = 0$$

$$B_1 p_{19} + C_1 p_{20} + D_1 p_{21} + E_1 p_{22} + F_1 p_{23} + \rho C_o + w F_o = 0$$

where:

$$p_1 = -1 - K_1 - \alpha E_o + \alpha \beta_2 E_{mo}$$

$$p_2 = -1 + \alpha K_2 + \alpha \beta_2 B_o$$

$$p_3 = -1 + \alpha \beta_2 B_o$$

$$p_4 = -1 + \alpha \beta_2 B_o + \beta_2 \beta \alpha K_2$$

$$p_5 = \alpha E_o$$

$$p_6 = -K_2 \alpha - \beta_o \gamma M$$

$$p_7 = \alpha B_o$$

$$p_8 = \beta_o \beta K_o \gamma$$

$$p_9 = -\delta E_{mo}$$

$$p_{10} = -\delta E_{mo} - \delta A_o$$

$$p_{11} = -\delta E_{mo} - \delta A_o - K_3 \delta - \xi$$

$$p_{12} = -\delta A_o$$

$$p_{13} = -\delta E_{mo} - \delta A_o + K_4 \xi$$

$$p_{14} = \alpha \beta_2 E_{mo}$$

$$p_{15} = -\alpha\beta_2 B_o + \beta_o\gamma M$$

$$p_{16} = -\alpha\beta_2 B_o + \xi$$

$$p_{17} = -\alpha\beta_2 B_o$$

$$p_{18} = -\alpha\beta_2 B_o - \beta\beta_2 K_2\alpha - K_4\xi - \beta_o\beta\gamma K_o$$

$$p_{19} = -\alpha E_o$$

$$p_{20} = -K_o\gamma + K_2\alpha$$

$$p_{21} = -K_o\gamma$$

$$p_{22} = -\gamma M - \gamma K_o - \alpha B_o$$

$$p_{23} = -K_o\gamma$$

And so we can solve the O(1) system:

$$A_1, B_1, C_1, D_1, F_1, E_1, E_{m1} = f(X_o, k_j^+, K_i, \beta_o, \beta_2)$$

where k_j^+ , $j = 0, 1, 2, 3, 4$ are the unknown forward rates, and X_o , $X = \{A, B, C, D, E, F, E_m\}$ are the equilibrium concentrations.

$$\begin{aligned} B_1 = & -((p_{11}p_4p_7 - p_3(p_{13}p_7 - p_{12}p_8))(p_4(-p_{22}p_6 + p_{20}p_7) - p_2(p_{23}p_7 - p_{22}p_8)) - (p_4(-p_{12}p_6 + \\ & p_{10}p_7) - p_2(p_{13}p_7 - p_{12}p_8))(p_{21}p_4p_7 - p_3(p_{23}p_7 - p_{22}p_8)))(- (p_{16}p_4p_7 - p_3(p_{18}p_7 - p_{17}p_8))(B_o(p_{13}p_7 - \\ & p_{12}p_8) + C_o p_{12}p_4\rho) + (p_{11}p_4p_7 - p_3(p_{13}p_7 - p_{12}p_8))(B_o(p_{18}p_7 - p_{17}p_8) + p_4(C_o p_{17}\rho - F_o p_7\omega))) + \\ & ((p_{11}p_4p_7 - p_3(p_{13}p_7 - p_{12}p_8))(p_4(-p_{17}p_6 + p_{15}p_7) - p_2(p_{18}p_7 - p_{17}p_8)) - (p_4(-p_{12}p_6 + p_{10}p_7) - \\ & p_2(p_{13}p_7 - p_{12}p_8))(p_{16}p_4p_7 - p_3(p_{18}p_7 - p_{17}p_8)))(- (p_{21}p_4p_7 - p_3(p_{23}p_7 - p_{22}p_8))(B_o(p_{13}p_7 - \\ & p_{12}p_8) + C_o p_{12}p_4\rho) + (p_{11}p_4p_7 - p_3(p_{13}p_7 - p_{12}p_8))(B_o(p_{23}p_7 - p_{22}p_8) + p_4(C_o p_{22}\rho + p_7(C_o r + \\ & F_o w)))))/(-((p_{11}p_4p_7 - p_3(p_{13}p_7 - p_{12}p_8))(p_4(-p_{22}p_6 + p_{20}p_7) - p_2(p_{23}p_7 - p_{22}p_8)) - (p_4(-p_{12}p_6 + \\ & p_{10}p_7) - p_2(p_{13}p_7 - p_{12}p_8))(p_{21}p_4p_7 - p_3(p_{23}p_7 - p_{22}p_8)))(p_{11}p_4p_7 - p_3(p_{13}p_7 - p_{12}p_8))(p_4(-p_{17}p_5 + \\ & p_{14}p_7) - p_1(p_{18}p_7 - p_{17}p_8)) - (p_{16}p_4p_7 - p_3(p_{18}p_7 - p_{17}p_8))(-p_1(p_{13}p_7 - p_{12}p_8) + p_4(-p_{12}p_5 + \\ & p_7p_9))) + ((p_{11}p_4p_7 - p_3(p_{13}p_7 - p_{12}p_8))(p_4(-p_{17}p_6 + p_{15}p_7) - p_2(p_{18}p_7 - p_{17}p_8)) - (p_4(-p_{12}p_6 + \\ & p_{10}p_7) - p_2(p_{13}p_7 - p_{12}p_8))(p_{16}p_4p_7 - p_3(p_{18}p_7 - p_{17}p_8)))(p_{11}p_4p_7 - p_3(p_{13}p_7 - p_{12}p_8))(p_4(-p_{22}p_5 + \\ & p_{19}p_7) - p_1(p_{23}p_7 - p_{22}p_8)) - (p_{21}p_4p_7 - p_3(p_{23}p_7 - p_{22}p_8))(-p_1(p_{13}p_7 - p_{12}p_8) + p_4(-p_{12}p_5 + p_7p_9)))), \end{aligned}$$

$$\begin{aligned} C_1 = & -(-B_o p_{13}p_{16}p_7 + B_o p_{11}p_{18}p_7 + B_o p_{12}p_{16}p_8 - B_o p_{11}p_{17}p_8 - C_o p_{13}p_{17}p_3\rho + C_o p_{12}p_{18}p_3\rho - \\ & C_o p_{12}p_{16}p_4\rho + C_o p_{11}p_{17}p_4\rho + F_o p_{13}p_3p_7\omega - F_o p_{11}p_4p_7\omega - F_o p_{12}p_3p_8\omega)/(p_{13}p_{17}p_3p_6 - p_{12}p_{18}p_3p_6 + \\ & p_{12}p_{16}p_4p_6 - p_{11}p_{17}p_4p_6 + p_{13}p_{16}p_2p_7 - p_{11}p_{18}p_2p_7 - p_{13}p_{15}p_3p_7 + p_{10}p_{18}p_3p_7 + p_1p_{15}p_4p_7 - \end{aligned}$$

$$\begin{aligned}
& p_{10}p_{16}p_4p_7 - p_{12}p_{16}p_2p_8 + p_{11}p_{17}p_2p_8 + p_{12}p_{15}p_3p_8 - p_{10}p_{17}p_3p_8) + (((p_{11}p_4p_7 - p_3(p_{13}p_7 - p_{12}p_8)) * \\
& (p_4(-p_{17}p_5 + p_{14}p_7) - p_1(p_{18}p_7 - p_{17}p_8)) - (p_{16}p_4p_7 - p_3(p_{18}p_7 - p_{17}p_8))(-p_1(p_{13}p_7 - p_{12}p_8) + \\
& p_4(-p_{12}p_5 + p_7p_9)))(-(p_{11}p_4p_7 - p_3(p_{13}p_7 - p_{12}p_8))(p_4(-p_{22}p_6 + p_{20}p_7) - p_2(p_{23}p_7 - p_{22}p_8)) - \\
& (p_4(-p_{12}p_6 + p_{10}p_7) - p_2(p_{13}p_7 - p_{12}p_8))(p_{21}p_4p_7 - p_3(p_{23}p_7 - p_{22}p_8)))(-(p_{16}p_4p_7 - p_3(p_{18}p_7 - \\
& p_{17}p_8))(B_o(p_{13}p_7 - p_{12}p_8) + C_o p_{12}p_4\rho) + (p_{11}p_4p_7 - p_3(p_{13}p_7 - p_{12}p_8))(B_o(p_{18}p_7 - p_{17}p_8) + \\
& p_4(C_o p_{17}\rho - F_o p_7\omega))) + ((p_{11}p_4p_7 - p_3(p_{13}p_7 - p_{12}p_8))(p_4(-p_{17}p_6 + p_{15}p_7) - p_2(p_{18}p_7 - p_{17}p_8)) - \\
& (p_4(-p_{12}p_6 + p_{10}p_7) - p_2(p_{13}p_7 - p_{12}p_8))(p_{16}p_4p_7 - p_3(p_{18}p_7 - p_{17}p_8)))(-(p_{21}p_4p_7 - p_3(p_{23}p_7 - \\
& p_{22}p_8))(B_o(p_{13}p_7 - p_{12}p_8) + C_o p_{12}p_4\rho) + (p_{11}p_4p_7 - p_3(p_{13}p_7 - p_{12}p_8))(B_o(p_{23}p_7 - p_{22}p_8) + \\
& p_4(C_o p_{22}\rho + p_7(C_o\rho + F_o\omega)))))/(((p_{11}p_4p_7 - p_3(p_{13}p_7 - p_{12}p_8))(p_4(-p_{17}p_6 + p_{15}p_7) - p_2(p_{18}p_7 - \\
& p_{17}p_8)) - (p_4(-p_{12}p_6 + p_{10}p_7) - p_2(p_{13}p_7 - p_{12}p_8))(p_{16}p_4p_7 - p_3(p_{18}p_7 - p_{17}p_8)))(-(p_{11}p_4p_7 - \\
& p_3(p_{13}p_7 - p_{12}p_8))(p_4(-p_{22}p_6 + p_{20}p_7) - p_2(p_{23}p_7 - p_{22}p_8)) - (p_4(-p_{12}p_6 + p_{10}p_7) - p_2(p_{13}p_7 - \\
& p_{12}p_8))(p_{21}p_4p_7 - p_3(p_{23}p_7 - p_{22}p_8)))(p_{11}p_4p_7 - p_3(p_{13}p_7 - p_{12}p_8))(p_4(-p_{17}p_5 + p_{14}p_7) - p_1(p_{18}p_7 - \\
& p_{17}p_8)) - (p_{16}p_4p_7 - p_3(p_{18}p_7 - p_{17}p_8))(-p_1(p_{13}p_7 - p_{12}p_8) + p_4(-p_{12}p_5 + p_7p_9))) + ((p_{11}p_4p_7 - \\
& p_3(p_{13}p_7 - p_{12}p_8))(p_4(-p_{17}p_6 + p_{15}p_7) - p_2(p_{18}p_7 - p_{17}p_8)) - (p_4(-p_{12}p_6 + p_{10}p_7) - p_2(p_{13}p_7 - \\
& p_{12}p_8))(p_{16}p_4p_7 - p_3(p_{18}p_7 - p_{17}p_8)))(p_{11}p_4p_7 - p_3(p_{13}p_7 - p_{12}p_8))(p_4(-p_{22}p_5 + p_{19}p_7) - p_1(p_{23}p_7 - \\
& p_{22}p_8)) - (p_{21}p_4p_7 - p_3(p_{23}p_7 - p_{22}p_8))(-p_1(p_{13}p_7 - p_{12}p_8) + p_4(-p_{12}p_5 + p_7p_9))))),
\end{aligned}$$

$$\begin{aligned}
D_1 = & -(B_o p_{13}p_{17}p_6 - B_o p_{12}p_{18}p_6 - B_o p_{13}p_{15}p_7 + B_o p_{10}p_{18}p_7 + B_o p_{12}p_{15}p_8 - B_o p_{10}p_{17}p_8 - \\
& C_o p_{13}p_{17}p_2\rho + C_o p_{12}p_{18}p_2\rho - C_o p_{12}p_{15}p_4\rho + C_o p_{10}p_{17}p_4\rho + F_o p_{12}p_4p_6\omega + F_o p_{13}p_2p_7\omega - F_o p_{10}p_4p_7\omega - \\
& F_o p_{12}p_2p_8\omega)/(-p_{13}p_{17}p_3p_6 + p_{12}p_{18}p_3p_6 - p_{12}p_{16}p_4p_6 + p_{11}p_{17}p_4p_6 - p_{13}p_{16}p_2p_7 + p_{11}p_{18}p_2p_7 + \\
& p_{13}p_{15}p_3p_7 - p_{10}p_{18}p_3p_7 - p_{11}p_{15}p_4p_7 + p_{10}p_{16}p_4p_7 + p_{12}p_{16}p_2p_8 - p_{11}p_{17}p_2p_8 - p_{12}p_{15}p_3p_8 + \\
& p_{10}p_{17}p_3p_8) + ((-p_{13}p_{17}p_2p_5 + p_{12}p_{18}p_2p_5 - p_{12}p_{15}p_4p_5 + p_{10}p_{17}p_4p_5 + p_1p_{13}p_{17}p_6 - p_1p_{12}p_{18}p_6 + \\
& p_{12}p_{14}p_4p_6 - p_1p_{13}p_{15}p_7 + p_1p_{10}p_{18}p_7 + p_{13}p_{14}p_2p_7 - p_{10}p_{14}p_4p_7 + p_1p_{12}p_{15}p_8 - p_1p_{10}p_{17}p_8 - \\
& p_{12}p_{14}p_2p_8 - p_{17}p_4p_6p_9 - p_{18}p_2p_7p_9 + p_{15}p_4p_7p_9 + p_{17}p_2p_8p_9)(-(p_{11}p_4p_7 - p_3(p_{13}p_7 - p_{12}p_8)) * \\
& (p_4(-p_{22}p_6 + p_{20}p_7) - p_2(p_{23}p_7 - p_{22}p_8)) - (p_4(-p_{12}p_6 + p_{10}p_7) - p_2(p_{13}p_7 - p_{12}p_8))(p_{21}p_4p_7 - \\
& p_3(p_{23}p_7 - p_{22}p_8)))(-(p_{16}p_4p_7 - p_3(p_{18}p_7 - p_{17}p_8)) * (B_o(p_{13}p_7 - p_{12}p_8) + C_o p_{12}p_4\rho) + (p_{11}p_4p_7 - \\
& p_3(p_{13}p_7 - p_{12}p_8)) * (B_o(p_{18}p_7 - p_{17}p_8) + p_4(C_o p_{17}\rho - F_o p_7\omega))) + ((p_{11}p_4p_7 - p_3(p_{13}p_7 - p_{12}p_8)) * \\
& (p_4(-p_{17}p_6 + p_{15}p_7) - p_2(p_{18}p_7 - p_{17}p_8)) - (p_4(-p_{12}p_6 + p_{10}p_7) - p_2(p_{13}p_7 - p_{12}p_8))(p_{16}p_4p_7 - \\
& p_3(p_{18}p_7 - p_{17}p_8)))(-(p_{21}p_4p_7 - p_3(p_{23}p_7 - p_{22}p_8))(B_o(p_{13}p_7 - p_{12}p_8) + C_o p_{12}p_4\rho) + (p_{11}p_4p_7 - \\
& p_3(p_{13}p_7 - p_{12}p_8))(B_o(p_{23}p_7 - p_{22}p_8) + p_4(C_o p_{22}\rho + p_7(C_o\rho + F_o\omega)))))/((p_{13}p_{17}p_3p_6 - p_{12}p_{18}p_3p_6 + \\
& p_{12} * p_{16}p_4p_6 - p_{11}p_{17}p_4p_6 + p_{13}p_{16}p_2p_7 - p_{11}p_{18}p_2p_7 - p_{13}p_{15}p_3p_7 + p_{10}p_{18}p_3p_7 + p_{11}p_{15}p_4p_7 - \\
& p_{10}p_{16}p_4p_7 - p_{12}p_{16}p_2p_8 + p_{11}p_{17}p_2p_8 + p_{12}p_{15}p_3p_8 - p_{10}p_{17}p_3p_8)(-(p_{11}p_4p_7 - p_3(p_{13}p_7 - p_{12}p_8)) * \\
& (p_4(-p_{22}p_6 + p_{20}p_7) - p_2(p_{23}p_7 - p_{22}p_8)) - (p_4(-p_{12}p_6 + p_{10}p_7) - p_2(p_{13}p_7 - p_{12}p_8))(p_{21}p_4p_7 - \\
& p_3(p_{23}p_7 - p_{22}p_8)))(p_{11}p_4p_7 - p_3(p_{13}p_7 - p_{12}p_8))(p_4(-p_{17}p_5 + p_{14}p_7) - p_1(p_{18}p_7 - p_{17}p_8)) - \\
& (p_{16}p_4p_7 - p_3(p_{18}p_7 - p_{17}p_8)) * (-p_1(p_{13}p_7 - p_{12}p_8) + p_4(-p_{12}p_5 + p_7p_9))) + ((p_{11}p_4p_7 - p_3(p_{13}p_7 - \\
& p_{12}p_8)) * (p_4(-p_{17}p_6 + p_{15}p_7) - p_2(p_{18}p_7 - p_{17}p_8)) - (p_4(-p_{12}p_6 + p_{10}p_7) - p_2(p_{13}p_7 - p_{12}p_8))(p_{16}p_4p_7 - \\
& p_3(p_{18}p_7 - p_{17}p_8)))(p_{11}p_4p_7 - p_3(p_{13}p_7 - p_{12}p_8)) * (p_4(-p_{22}p_5 + p_{19}p_7) - p_1(p_{23}p_7 - p_{22}p_8)) -
\end{aligned}$$

$$(p_{21}p_4p_7 - p_3(p_{23}p_7 - p_{22}p_8))(-p_1(p_{13}p_7 - p_{12}p_8) + p_4(-p_{12}p_5 + p_7p_9))))) ,$$

$$\begin{aligned} E_1 = & -(-B_o p_{13}p_{16}p_6 + B_o p_{11}p_{18}p_6 - B_o p_{11}p_{15}p_8 + B_o p_{10}p_{16}p_8 + C_o p_{13}p_{16}p_2\rho - C_o p_{11}p_{18}p_2\rho - \\ & C_o p_{13}p_{15}p_3\rho + C_o p_{10}p_{18}p_3\rho + C_o p_{11}p_{15}p_4\rho - C_o p_{10}p_{16}p_4\rho + F_o p_{13}p_3p_6\omega - F_o p_{11}p_4p_6\omega + F_o p_{11}p_2p_8\omega - \\ & F_o p_{10}p_3p_8\omega)/(-p_{13}p_{17}p_3p_6 + p_{12}p_{18}p_3p_6 - p_{12}p_{16}p_4p_6 + p_{11}p_{17}p_4p_6 - p_{13}p_{16}p_2p_7 + p_{11}p_{18}p_2p_7 + \\ & p_{13}p_{15}p_3p_7 - p_{10}p_{18}p_3p_7 - p_{11}p_{15}p_4p_7 + p_{10}p_{16}p_4p_7 + p_{12}p_{16}p_2p_8 - p_{11}p_{17}p_2p_8 - p_{12}p_{15}p_3p_8 + \\ & p_{10}p_{17}p_3p_8) + ((-p_{13}p_{16}p_2p_5 + p_{11}p_{18}p_2p_5 + p_{13}p_{15}p_3p_5 - p_{10}p_{18}p_3p_5 - p_{11}p_{15}p_4p_5 + p_{10}p_{16}p_4p_5 + \\ & p_{11}p_{13}p_{16}p_6 - p_{11}p_{11}p_{18}p_6 - p_{13}p_{14}p_3p_6 + p_{11}p_{14}p_4p_6 + p_{11}p_{11}p_{15}p_8 - p_{11}p_{10}p_{16}p_8 - p_{11}p_{14}p_2p_8 + \\ & p_{10}p_{14}p_3p_8 + p_{18}p_3p_6p_9 - p_{16}p_4p_6p_9 + p_{16}p_2p_8p_9 - p_{15}p_3p_8p_9)(-(p_{11}p_4p_7 - p_3(p_{13}p_7 - p_{12}p_8)) * \\ & (p_4(-p_{22}p_6 + p_{20}p_7) - p_2(p_{23}p_7 - p_{22}p_8)) - (p_4(-p_{12}p_6 + p_{10}p_7) - p_2(p_{13}p_7 - p_{12}p_8))(p_{21}p_4p_7 - \\ & p_3(p_{23}p_7 - p_{22}p_8)))(-(p_{16}p_4p_7 - p_3(p_{18}p_7 - p_{17}p_8))(B_o(p_{13}p_7 - p_{12}p_8) + C_o p_{12}p_4\rho) + (p_{11}p_4p_7 - \\ & p_3(p_{13}p_7 - p_{12}p_8)) * (B_o(p_{18}p_7 - p_{17}p_8) + p_4(C_o p_{17}\rho - F_o p_7\omega))) + ((p_{11}p_4p_7 - p_3(p_{13}p_7 - p_{12}p_8)) * \\ & (p_4(-p_{17}p_6 + p_{15}p_7) - p_2(p_{18}p_7 - p_{17}p_8)) - (p_4(-p_{12}p_6 + p_{10}p_7) - p_2(p_{13}p_7 - p_{12}p_8))(p_{16}p_4p_7 - \\ & p_3(p_{18}p_7 - p_{17}p_8)))(-(p_{21}p_4p_7 - p_3(p_{23}p_7 - p_{22}p_8))(B_o(p_{13}p_7 - p_{12}p_8) + C_o p_{12}p_4\rho) + (p_{11}p_4p_7 - \\ & p_3(p_{13}p_7 - p_{12}p_8))(B_o(p_{23}p_7 - p_{22}p_8) + p_4(C_o p_2\rho + p_7(C_o\rho + F_o\omega)))))))/((-p_{13}p_{17}p_3p_6 + p_{12}p_{18}p_3p_6 - \\ & p_{12}p_{16}p_4p_6 + p_{11}p_{17}p_4p_6 - p_{13}p_{16}p_2p_7 + p_{11}p_{18}p_2p_7 + p_{13}p_{15}p_3p_7 - p_{10}p_{18}p_3p_7 - p_{11}p_{15}p_4p_7 + \\ & p_{10}p_{16}p_4p_7 + p_{12}p_{16}p_2p_8 - p_{11}p_{17}p_2p_8 - p_{12}p_{15}p_3p_8 + p_{10}p_{17}p_3p_8) * (-((p_{11}p_4p_7 - p_3(p_{13}p_7 - \\ & p_{12}p_8))(p_4(-p_{22}p_6 + p_{20}p_7) - p_2(p_{23}p_7 - p_{22}p_8)) - (p_4(-p_{12}p_6 + p_{10}p_7) - p_2(p_{13}p_7 - p_{12}p_8))(p_{21}p_4p_7 - \\ & p_3(p_{23}p_7 - p_{22}p_8))) * ((p_{11}p_4p_7 - p_3(p_{13}p_7 - p_{12}p_8)) * (p_4(-p_{17}p_6 + p_{15}p_7) - p_1(p_{18}p_7 - p_{17}p_8)) - \\ & (p_{16}p_4p_7 - p_3(p_{18}p_7 - p_{17}p_8))(-p_1(p_{13}p_7 - p_{12}p_8) + p_4(-p_{12}p_5 + p_7p_9))) + ((p_{11}p_4p_7 - p_3(p_{13}p_7 - \\ & p_{12}p_8)) * (p_4(-p_{17}p_6 + p_{15}p_7) - p_2(p_{18}p_7 - p_{17}p_8)) - (p_4(-p_{12}p_6 + p_{10}p_7) - p_2(p_{13}p_7 - p_{12}p_8))(p_{16}p_4p_7 - \\ & p_3(p_{18}p_7 - p_{17}p_8)))(p_{11}p_4p_7 - p_3(p_{13}p_7 - p_{12}p_8))(p_4(-p_{22}p_5 + p_{19}p_7) - p_1(p_{23}p_7 - p_{22}p_8)) - \\ & (p_{21}p_4p_7 - p_3(p_{23}p_7 - p_{22}p_8))(-p_1(p_{13}p_7 - p_{12}p_8) + p_4(-p_{12}p_5 + p_7p_9))))) , \end{aligned}$$

$$\begin{aligned} F_1 = & -(B_o p_{12}p_{16}p_6 - B_o p_{11}p_{17}p_6 + B_o p_{11}p_{15}p_7 - B_o p_{10}p_{16}p_7 - C_o p_{12}p_{16}p_2\rho + C_o p_{11}p_{17}p_2\rho + \\ & C_o p_{12}p_{15}p_3\rho - C_o p_{10}p_{17}p_3\rho - F_o p_{12}p_3p_6\omega - F_o p_{11}p_2p_7\omega + F_o p_{10}p_3p_7\omega)/(-p_{13}p_{17}p_3p_6 + p_{12}p_{18}p_3p_6 - \\ & p_{12}p_{16}p_4p_6 + p_{11}p_{17}p_4p_6 - p_{13}p_{16}p_2p_7 + p_{11}p_{18}p_2p_7 + p_{13}p_{15}p_3p_7 - p_{10}p_{18}p_3p_7 - p_{11}p_{15}p_4p_7 + \\ & p_{10}p_{16}p_4p_7 + p_{12}p_{16}p_2p_8 - p_{11}p_{17}p_2p_8 - p_{12}p_{15}p_3p_8 + p_{10}p_{17}p_3p_8) + ((p_{12}p_{16}p_2p_5 - p_{11}p_{17}p_2p_5 - \\ & p_{12}p_{15}p_3p_5 + p_{10}p_{17}p_3p_5 - p_{11}p_{12}p_{16}p_6 + p_{11}p_{11}p_{17}p_6 + p_{12}p_{14}p_3p_6 - p_{11}p_{11}p_{15}p_7 + p_{11}p_{10}p_{16}p_7 + \\ & p_{11}p_{14}p_2p_7 - p_{10}p_{14}p_3p_7 - p_{11}p_{17}p_3p_6p_9 - p_{16}p_2p_7p_9 + p_{15}p_3p_7p_9)(-(p_{11}p_4p_7 - p_3(p_{13}p_7 - p_{12}p_8)) * \\ & (p_4(-p_{22}p_6 + p_{20}p_7) - p_2(p_{23}p_7 - p_{22}p_8)) - (p_4(-p_{12}p_6 + p_{10}p_7) - p_2(p_{13}p_7 - p_{12}p_8))(p_{21}p_4p_7 - \\ & p_3(p_{23}p_7 - p_{22}p_8)))(-(p_{16}p_4p_7 - p_3(p_{18}p_7 - p_{17}p_8))(B_o(p_{13}p_7 - p_{12}p_8) + C_o p_{12}p_4\rho) + (p_{11}p_4p_7 - \\ & p_3(p_{13}p_7 - p_{12}p_8))(B_o(p_{18}p_7 - p_{17}p_8) + p_4(C_o p_{17}\rho - F_o p_7\omega))) + ((p_{11}p_4p_7 - p_3(p_{13}p_7 - p_{12}p_8)) * \\ & (p_4(-p_{17}p_6 + p_{15}p_7) - p_2(p_{18}p_7 - p_{17}p_8)) - (p_4(-p_{12}p_6 + p_{10}p_7) - p_2(p_{13}p_7 - p_{12}p_8))(p_{16}p_4p_7 - \\ & p_3(p_{18}p_7 - p_{17}p_8)))(-(p_{21}p_4p_7 - p_3(p_{23}p_7 - p_{22}p_8))(B_o(p_{13}p_7 - p_{12}p_8) + C_o p_{12}p_4\rho) + (p_{11}p_4p_7 - \\ & p_3(p_{13}p_7 - p_{12}p_8))(B_o(p_{23}p_7 - p_{22}p_8) + p_4(C_o p_2\rho + p_7(C_o\rho + F_o\omega)))))))/((-p_{13}p_{17}p_3p_6 + p_{12}p_{18}p_3p_6 - \\ & p_{12}p_{16}p_4p_6 + p_{11}p_{17}p_4p_6 - p_{13}p_{16}p_2p_7 + p_{11}p_{18}p_2p_7 + p_{13}p_{15}p_3p_7 - p_{10}p_{18}p_3p_7 - p_{11}p_{15}p_4p_7 + \end{aligned}$$

$$\begin{aligned}
& p_{10}p_{16}p_4p_7 + p_{12}p_{16}p_2p_8 - p_{11}p_{17}p_2p_8 - p_{12}p_{15}p_3p_8 + p_{10}p_{17}p_3p_8) - ((p_{11}p_4p_7 - p_3(p_{13}p_7 - p_{12}p_8)) * \\
& (p_4(-p_{22}p_6 + p_{20}p_7) - p_2(p_{23}p_7 - p_{22}p_8)) - (p_4(-p_{12}p_6 + p_{10}p_7) - p_2(p_{13}p_7 - p_{12}p_8))(p_{21}p_4p_7 - \\
& p_3(p_{23}p_7 - p_{22}p_8)))((p_{11}p_4p_7 - p_3(p_{13}p_7 - p_{12}p_8))(p_4(-p_{17}p_5 + p_{14}p_7) - p_1(p_{18}p_7 - p_{17}p_8)) - \\
& (p_{16}p_4p_7 - p_3(p_{18}p_7 - p_{17}p_8))(-p_1(p_{13}p_7 - p_{12}p_8) + p_4(-p_{12}p_5 + p_7p_9))) + ((p_{11}p_4p_7 - p_3(p_{13}p_7 - \\
& p_{12}p_8))(p_4(-p_{17}p_6 + p_{15}p_7) - p_2(p_{18}p_7 - p_{17}p_8)) - (p_4(-p_{12}p_6 + p_{10}p_7) - p_2(p_{13}p_7 - p_{12}p_8))(p_{16}p_4p_7 - \\
& p_3(p_{18}p_7 - p_{17}p_8)))((p_{11}p_4p_7 - p_3(p_{13}p_7 - p_{12}p_8))(p_4(-p_{22}p_5 + p_{19}p_7) - p_1(p_{23}p_7 - p_{22}p_8)) - \\
& (p_{21}p_4p_7 - p_3(p_{23}p_7 - p_{22}p_8))(-p_1(p_{13}p_7 - p_{12}p_8) + p_4(-p_{12}p_5 + p_7p_9))))).
\end{aligned}$$

We now calculate the fluxes through each pathway of the full model. We first label the fluxes as follows:

$$A \xrightarrow{f_1} B \xrightarrow{f_2} C \xrightarrow{f_3} F \xrightarrow{g_3} \text{ where } f_3 = \text{CS pathway flux}$$

$$A \xrightarrow{f_5} D \xrightarrow{f_5} F \xrightarrow{g_3} \text{ where } f_5 = \text{Standard Pathway flux}$$

$$B \xrightarrow{f_4} F \xrightarrow{g_3} \text{ where } f_4 = \text{Alternate Pathway flux}$$

$$B \xrightarrow{g_1} A$$

$$C \xrightarrow{g_2} A$$

We have the following system of equations, where $g_1 = h_1B$, $g_2 = h_2C$, $g_3 = h_3F$.

$$f_1 = f_4 + f_2 + g_1$$

$$f_2 = f_3 + g_2$$

$$f_3 + f_4 + f_5 = g_3$$

Then all fluxes can be written in terms of fluxes f_2 , f_4 :

$$f_1 = g_1 + f_2 + f_4$$

$$f_3 = f_2 - g_2$$

$$f_5 = g_3 - f_4 - f_3$$

We can write the fluxes f_2 , f_4 as the following differences:

$$f_2 = k_2^+ BE - k_2^- C$$

$$f_4 = \beta_2 k_2^+ BE_m - \beta_2 \beta k_2^- F$$

Substitution of our asymptotic solutions gives the following approximation of the fluxes at steady state:

$$f_2 = k_2^+(B_o + \epsilon B_1)(E_o + \epsilon E_1) - k_2^-(C_o + \epsilon C_1)$$

$$f_4 = \beta_2 k_2^+(B_o + \epsilon B_1)(E_{m_o} + \epsilon E_{m_1}) - \beta_2 \beta k_2^-(F_o + \epsilon F_1).$$